MATHEMATICS IN ENGINEERING, SCIENCE AND AEROSPACE
MESA - www.journalmesa.com
Vol. 8, No. 4, pp. 431-474, 2017

Analytical and experimental probabilistic constitutive relation characterizations, part I: linear viscoelastic media

Harry H. Hilton [1*], Jutima Simsiriwong [2], Rani Warsi Sullivan [3]

[1] Aerospace Engineering Department, College of Engineering and Computing
and Data Sciences Division, National Center for Supercomputing Applications
University of Illinois at Urbana-Champaign, Urbana, IL 61801-2935 USA
Professor Emeritus of Aerospace Engineering and Senior Academic Lead for Computational Structural/Solid Mechanics at NCSA.
Voice: 217-333-2653 Cell: 217-840-1116 FAX: 217-244-0720 E-mail: h-hilton@illinois.edu

[2] Mechanical Engineering Department, Auburn University, Auburn, AL 36849 USA
Visiting Assistant Professor of Mechanical Engineering,
Voice: 334-844-4820 E-mail:jutima@auburn.edu

[3] Aerospace Engineering Department
Mississippi State University, Mississippi State, MS 39762 USA
Associate Professor of Aerospace Engineering.
Voice: 662-325-7289 E-mail: sullivan@msstate.edu

[*] *Corresponding Author*. E-mail: h-hilton@illinois.edu

Abstract. Analytical and experimental deterministic and statistical protocols are formulated for the constitutive linear relations that characterize viscoelastic media. These proceedings are achieved in the real time space in terms of moduli and/or compliances without any inclusion of viscoelastic Poisson's ratios. Independent experimental determinations of linear viscoelastic material properties of three distinct polymers include single conditions of creep, relaxation, and constant strain and extensometer time rates - except for starting transients.

Statistical dynamic data for the instantaneous modulus and quasi-static data for relaxation moduli are analytically and numerically merged to produce relaxation modulus and creep compliance expressions containing properly evaluated parameters. The combined actual starting load and displacement transient and subsequent time histories are tracked, recorded and incorporated into the analyses to produce moduli and compliances based on actual continuous loading-time sequences.

[2010] **Mathematics Subject Classification**: 35G05, 35G10, 35Q74, 45C05, 45F15, 45K05.
Keywords: analytical and experimental characterization, deterministic, stochastic, quasi-static and dynamic experiments, spectral formulations, viscoelasticity, vinyl ester polymer .

Prony series and generalized continuous relaxation time spectral modulus and compliance functions are derived and discussed. Four distinct probability models of material properties and temperature are postulated and evaluated for two sets of real viscoelastic materials (polymers). Statistical sufficiency considerations are included in the analyses.

1 Introduction

Viscoelasticity has found many theoretical and practical applications ranging from high polymer composites, solid propellants, aero-viscoelasticity, high temperature metals, ice, in-vivo tissue, foods, to mention but a few materials and their impact [1 – 30]. The present paper combines various theoretical and experimental aspects leading to the characterization of relaxation moduli and creep compliances common to all viscoelastic materials.

Since the middle of the last century the aerospace industry has made use of structural probability concepts based on the so-called A and B values of Ref. [31], albeit sometimes reluctantly and in other instances inadvertently.[1] However, in a field where minimum structural weight and high efficiency performance of flight structures are de facto primary requirements, the necessity of including structural probability is paramount[2] [32], [33]. Structural material characterization manifests itself in two distinct forms, namely constitutive relations and failure criteria. This paper addresses only the first property class, but it is a relatively simple task to extend the developed protocols to the second set of criteria [34] such as the empirical rules of [32], [33], which include probability concepts.

Viscoelastic material properties are notorious for their highly scattered values. Such wide dispersions, compared to elastic material behavior, are fundamentally due to past and continuing inabilities to properly manufacture time-dependent materials to any strict tolerances. Hence, with the current and predicted heavy reliance on high polymer composites, biological materials, etc., statistical data collections and probabilistic analyses appear mandatory.

Additionally and independently, applied loads, displacements and temperatures as well as geometries and their dimensions are non-deterministic. Random gust loads have long been an ongoing analysis concern on flight vehicles, buildings, bridges, etc., [35]. Because of the extreme sensitivity of viscoelastic media to temperature variations,[3] and due to their frequent statistical occurrences [36], the influence of random temperatures has been included in the present analyses.

The ever pervasive requirements of proper material characterization can only be achieved through systematic high fidelity experimentations of relatively simple but extremely meaningful tests that can be completely reproduced and solved analytically. To that end, the experiments and analyses treated herein are deliberately limited to isotropic homogeneous 1–D dynamic and quasi-static phenomena.

The required statistical and probability theories needed for the current studies are well established and covered in studies such as Refs. [37 – 47]. A few examples of random structural elastic and viscoelastic analyses and experimentations are covered in [48 – 62]. The most common probabilistic structural applications have involved failure conditions with only a few treatments of constitutive relations.

[1] The Army-Navy ANC-5 Bulletin was originally published in 1937 and has undergone numerous revisions since then. These A and B "ultimate" stress values refer to 0.90 and 0.95 probability of failure values.

[2] Based on the Shanley-Ryder [34] stress ratio failure theory. There are, of course, numerous other deterministic approaches.

[3] Roughly one order of magnitude change in the viscoelastic viscosity coefficients per 20℃, see Fig. 6.

Continuous spectral representations have been treated extensively in [63 – 72] and offer an alternative characterization of viscoelastic moduli and compliances. Generalized expressions for arbitrary continuous spectral functions are derived and evaluated.

It is planned to follow up this paper by a subsequent one treating nonlinear viscoelastic random characterizations [73].

2 NOMENCLATURE

Abbreviations

BC, IC	boundary and initial condition
BVP, IVP	boundary and initial value problem
CDF	cumulative distribution function
FD	fractional derivative
GKM, KM	generalized Kelvin model and single Kelvin model
iff	if and only if
l.h.s., r.h.s.	left and right hand side
LN	log – normal
LSQ	least squares method
LT, FT	Laplace and Fourier transforms
PDF	probability density function
qs, QS	quasi static conditions and responses
SEVCP, EVCP	stochastic and deterministic elastic-viscoelastic correspondence principle
TSM	thermo-rheologically simple material
VER	vinyl ester resin

Symbols

$a_T(t)$	WLF shift function
A	area
$B[\alpha(t),\beta(t)]$	complete beta function
$\mathscr{BL}$	bilateral LT
c,h,L	coupon cross-sectional dimensions, width and thickness, and length
C_{ijkl}	creep compliances
$\boldsymbol{E}$	expected value
E,E_{ijkl}	relaxation moduli
E^e,E^0	elastic Young's modulus
E^τ	spectral shape function
E^{SP}	spectral modulus
$F(t)$	applied tension force
$\mathscr{F},\mathscr{L}$	Fourier and Laplace transfrom
I	moment of inertia
$\boldsymbol{I}=\{I_1,I_2,I_3\}$	strain invariant set
I_i	strain invariants
L_0	original specimen length
O	order of
$Pr(\widetilde{y})$	probability of $\widetilde{y}$ occurrence

$\mathbb{R}_{\mathbb{U}}\ \mathbb{R}_{\mathbb{SI}}$	positive unit $[0,\ 1]$ and semi-infinite space $[0,\ \infty]$
SUF	sufficiency parameter
t	time
T	temperature
$[Ti]$	time dimension
u_i	displacement component
$x_i,\ x = \{x_1, x_2, x_3\}$	Cartesian coordinate
δ_{ij}	Kronecker delta
ε	mean strain
ε_{ij}	strain components
$\Gamma[Z(t)]$	gamma function
σ	mean stress
σ_{ij}	stresses in x_i direction
σ_{12}	shear stresses
σ_{SD}	standard deviation
τ_{ijkl}	relaxation times
τ^*_{ijkl}	$= 1/\tau_{ijkl}$
θ	angle of twist
ω	FT frequency

Notes: Numbers in parentheses refer to equations, whereas square brackets indicate references.
A $\widetilde{}$ over a symbol designates a random variable or function.
A $\widehat{}$ over a symbol designates a matrix member.
All stresses and moduli are in MPa units.

3 ANALYSIS I: ISOTHERMAL CONDITIONS

3.1 General considerations

In principle, for both isothermal and variable temperature conditions, nature presents deterministic and random events with or without complete sets of random variables[4] and events, such as state variables including temperature, material properties, boundary and initial conditions. In the analysis to follow a number of such states will be isolated and examined in detail. In particular, deterministic events will be considered first and then their stochastic cousins will be analyzed through the former's random reconstructions.

In the present study the main focus is on linear viscoelastic material characterization (moduli, compliances, shift functions) and not on random applied loads, BCs or ICs [32], [33], which with the exception of temperature will be considered deterministic. The resultant stochastic stresses, strains and displacements are, therefore, the consequences of the random material properties.

3.1.1 *The random variables*

Let $\widetilde{X}$ be a set of dimensioned random variables, while $\widetilde{X}_W$, $\widetilde{X}_{LN}$, $\widetilde{X}_G$ and $\widetilde{X}_B$ respectively are dimensionless Weibull, log-normal, Gauss and beta random variables. The mathematical expressions for

[4] Random variables are denoted by a superior tilde ($\widetilde{\sigma}_{ij}$).

the numerous probability density functions (PDF) are self consistent and operationally follow well established rules rigorously proven by numerous theorems. They differ in purpose, shape and utility. In many instances their departure from the real physical world can be profound.

Case in point: the operational space (interval) over which each distinct PDF is defined. These intervals, which are implicit to each designated PDF, range from infinite $[-\infty, \infty]$ (Gauss) through semi-infinite $[0, \infty]$ (Weibull, log-normal) to finite $[0, 1]$ (beta)[5]. Real world random physical state variables have beginning and ending finite values at each unique combination of t_a and $T_b(x,t_a)$, such as X_{min} and X_{max}. These serve to make dimensionless the variables specifically associated with each distribution.

Consequently at each time t and temperature $T(x,t)$, one needs to define the following dimensionless variables

$$\underbrace{\widetilde{y}}_{\substack{\text{general}\\ \text{variable}}} = \underbrace{\left\{\begin{array}{c}\widetilde{X}_W\\ \widetilde{X}_B\\ \widetilde{X}_{LN}\\ \widetilde{X}_G\\ \vdots\end{array}\right\}}_{\text{specific PDF}} = \underbrace{\frac{\widetilde{X} - X_{min}\left[x,t_a;T_b(x,t_a)\right]}{X_{max}\left[x,t_a;T(x,t_b)\right] - X_{min}\left[x,t_a;T_b(x,t_a)\right]}}_{\text{non-dimensialization of physical variables}} \text{ with } \left\{\begin{array}{l}\widetilde{y} \in [0,\,1]\\ \\ \widetilde{X} \in [X_{min}, X_{max}]\end{array}\right. \tag{3.1}$$

These dimensionless variables operate in the unit interval $0 \to 1$, whereas the actual physical ones $\widetilde{X}$ extend from their own $X_{min}\left[x,t_a;T_b(x,t_a)\right]$ to their corresponding $X_{max}\left[x,t_a;T_b(x,t_a)\right]$. Additionally, the individual mean and variance values, and the PDF parameters must be similarly non-dimensionalized.

The non-zero beta PDF extends only over the range $\mathbb{R}_{\mathbb{U}}$, while most other PDFs, in principle, cover the positive infinite half space, except the likes of the Gauss PDF which ranges from $-\infty$ to ∞.

Statistical experimental data [50] strongly indicates the relaxation modulus curves obtained from various experiments take on random shapes and may cross each other in time on one or more occasions. Consequently the PDF parameter must be considered to be time–temperature functions.

However, statistical viscoelastic experiments are generally conducted at constant temperatures and, therefore, $T_b(x,t_a) = \{T_1, T_2, \cdots\}$ represents the set of constant temperatures at which the data was collected.

The operational steps for normalizing data and PDF variables and for determining pertinent parameters for each selected time and temperature pair are

1 - normalize the statistical data according to Eq. (3.1)

2 - compute means and variances of the normalized data for each t and T pair

3 - compute parameters for the Weibull and beta PDFs from these means and variances[6] – Eqs. (3.9) to (3.19)

4 - alternately, PDF parameters may be computed through LSQ fits of each PDF or by matching statistical moments at constant times and temperatures

5 the PDFs and CDFs graphs, Figs. 1 to 3 and 16 to 18, are then generated using the established parameters and plotted against $\widetilde{y} \in [0,\ 1]$

6 - for either protocol 3 and 4, PDF parameter time and temperature functions are established through an additional LSQ fit in the temperature space

Of course, the enduring question always remains: Has one conducted a sufficient number of experiments and obtained an adequate number of statistical samples to capture high fidelity minimum

[5] Only single examples are noted. See [37 – 49] for additional PDFs.

[6] Log-normal and Gauss parameters are these means and variances

and maximum values for the ensemble of test data as well as perform meaningful PDF curve fittings? Fortunately, modern statistical theories offer rigorous responses to this query [45 – 47]. A few of these statistical sufficiencies are[7]

$$\text{Weibull PDF} \implies SUF_W(t) = \prod_{n=1}^{N_{SUF}^W} \left(\frac{\widetilde{y}_n}{\lambda(t)}\right)^{k(t)-1} \prod_{n=1}^{N_{SUF}^W} \exp\left[-\left(\frac{\widetilde{y}_n}{\lambda(t)}\right)^{k(t)}\right] \tag{3.2}$$

$$\log-\text{normal PDF} \implies SUF_{LN}(t) = \prod_{n=1}^{N_{SUF}^{LN}} \frac{1}{\widetilde{y}_n} \prod_{n=1}^{N_{SUF}^{LN}} \exp\left[-\left(\frac{\ln(\widetilde{y}_n)-\mu(t)}{\sqrt{2}\,\sigma_{ST}(t)}\right)^2\right] \tag{3.3}$$

$$\text{Gauss PDF} \implies SUF_G(t) = \prod_{n=1}^{N_{SUF}^G} \exp\left[-\left(\frac{\widetilde{y}_n-\mu(t)}{\sqrt{2}\,\sigma_{ST}(t)}\right)^2\right] \tag{3.4}$$

$$\text{beta PDF} \implies SUF_B(t) = \prod_{n=1}^{N_{SUF}^B} \widetilde{y}_n^{\alpha(t)-1} \prod_{n=1}^{N_{SUF}^B} (1-\widetilde{y}_n)^{\beta(t)-1} \tag{3.5}$$

$$\text{with} \quad \widetilde{y} \in \mathbb{R}_{\mathbb{U}} \in [0,\ 1] \ \text{ or } \ \mathbb{R}_{\mathbb{SI}} \in [0,\ \infty] \ \text{ and } \ t \in [0,\ \infty] \tag{3.6}$$

All parameters in the PDFs are time and temperature-dependent, i.e. $k(t) \equiv k[t;T(t)]$, etc.

$SUF(t) \equiv SUF[t;T(t)]$ is said to be sufficient if and only if the latter is independent of the $\widetilde{y}_n$ distributions. In a practical sense this means that for a chosen PDF, the number of samples N_{SUF} is large enough for the product series of the type (3.2) to (3.5) to "converge" numerically. Numerical "convergence" is defined here to occur when SUF remains substantially unchanged[8] between $N_{SUF}-1$ and N_{SUF} samples, or

$$\text{error}_{\text{SUF}}(\text{t}) = \frac{\text{SUF}(\text{t};\text{N}_{\text{SUF}}) - \text{SUF}(\text{t};\text{N}_{\text{SUF}}-1)}{\text{SUF}(\text{t};\text{N}_{\text{SUF}})} \ll 1 \tag{3.7}$$

Formally, moduli are defined in the half infinite space $0 \le t \le t_R \le \infty$, see Fig. 4. However, it is conceivable that some of the experimental data may be gathered in a time interval shorter than t_R due to specimen and/or equipment failures or too long a time period for practical data gathering. In those cases the number of data points will be time-dependent, i.e. a piecewise function $N(t)$ that varies with each experiment.

3.1.2 *The Weibull, log-normal, Gauss and beta probability distributions (PDF & CDF)*

It is necessary to separate and differentiate between each of the following: deterministic or stochastic stresses, material properties, temperatures, etc., analytical and experimental results.

For example, consider four PDFs, the Weibull and log-normal ones in a positive semi-infinite interval $\mathbb{R}_{\mathbb{SI}}$, the Gauss one in an infinite interval $[-\infty,\ \infty]$ and the beta PDF in a positive finite unit interval $\mathbb{R}_{\mathbb{U}}$, with a

$$\text{mean} \implies \mu(t) = \frac{1}{N_y}\sum_{n=1}^{N_y}\widetilde{y}_n, \qquad \left.\begin{array}{ll} (\text{standard deviation})^2 \implies [\sigma_{SD}(t)]^2 \\ \text{variance} \implies \boldsymbol{Var}(\widetilde{y}) \end{array}\right\} = \frac{1}{N_y}\sum_{n=1}^{N_y}[\widetilde{y}_n-\mu(t)]^2 \tag{3.8}$$

[7] Note the association between various parameters and specific PDFs.

[8] as specified by the desired number of significant figures in the difference between the last two terms of the products and evaluated by (3.7)

calculated from the $\widetilde{y}_n$ experimental data points. Their PDFs and CFDs then are [49], [74], [75]

$$\left.\begin{array}{c}\text{Weibull PDF} \Longrightarrow \\ \widetilde{\phi}_W\left[\widetilde{y};\lambda(t),k(t)\right]\end{array}\right\} = \begin{cases} \dfrac{k(t)}{\lambda(t)}\left(\dfrac{\widetilde{y}}{\lambda(t)}\right)^{k(t)-1}\exp\left[-\left(\dfrac{\widetilde{y}}{\lambda(t)}\right)^{k(t)}\right] & \widetilde{y}\in\mathbb{R}_{\mathbb{SI}} \\ 0 & \widetilde{y}\notin\mathbb{R}_{\mathbb{SI}} \end{cases} \tag{3.9}$$

$$\left.\begin{array}{c}\text{Weibull CDF} \Longrightarrow \\ Pr_W\left[\widetilde{y};\lambda(t),k(t)\right] \\ \displaystyle\int_0^{\widetilde{y}}\widetilde{\phi}_W\left[Y;\lambda(t),k(t)\right]\,dY\end{array}\right\} = \begin{cases} 1-\exp\left[-\left(\dfrac{\widetilde{y}}{\lambda(t)}\right)^{k(t)}\right] & \widetilde{y}\in\mathbb{R}_{\mathbb{SI}} \\ 0 & \widetilde{y}\notin\mathbb{R}_{\mathbb{SI}} \end{cases} \quad \lambda(t),k(t)>0 \tag{3.10}$$

The Weibull parameters are related to the first two statistical moments by

$$\mu(t) = \lambda(t)\,\Gamma\left[1+\frac{1}{k(t)}\right] \qquad \text{and} \qquad \left[\sigma_{SD}(t)\right]^2 = \left[\lambda(t)\right]^2\left[\Gamma\left(1+\frac{2}{k(t)}\right)-\left[\Gamma\left(1+\frac{1}{k(t)}\right)\right]^2\right] \tag{3.11}$$

$$\left.\begin{array}{c}\log-\text{normal PDF} \Longrightarrow \\ \widetilde{\phi}_{LN}\left[\widetilde{y};\mu_{LN}(t),\sigma_{LN}(t)\right]\end{array}\right\} = \begin{cases} \dfrac{1}{\widetilde{y}\,\sigma_{LN}(t)\sqrt{2\pi}}\exp\left(-\left[\dfrac{\ln(\widetilde{y})-\mu_{LN}(t)}{\sqrt{2}\,\sigma_{LN}(t)}\right]^2\right) & \widetilde{y}\in\mathbb{R}_{\mathbb{SI}} \\ 0 & \widetilde{y}\notin\mathbb{R}_{\mathbb{SI}} \end{cases} \tag{3.12}$$

$$\left.\begin{array}{c}\log-\text{normal CDF} \Longrightarrow \\ Pr_{LN}\left[\widetilde{y};\mu_{LN}(t),\sigma_{LN}(t)\right] \\ \displaystyle\int_0^{\widetilde{y}}\widetilde{\phi}_{LN}\left[Y;\mu_{LN}(t),\sigma_{LN}(t)\right]\,dY\end{array}\right\} = \begin{cases} \dfrac{1}{2}\left[1+\operatorname{erf}\underbrace{\left(\dfrac{\ln(\widetilde{y})-\mu_{LN}(t)}{\sqrt{2}\,\sigma_{LN}(t)}\right)}_{=Z(t)}\right] & \widetilde{y}\in\mathbb{R}_{\mathbb{SI}} \\ 0 & \widetilde{y}\notin\mathbb{R}_{\mathbb{SI}} \end{cases} \tag{3.13}$$

where the parameters μ_{LN} and σ_{LN} are associated with the mean and standard deviation of $\ln(\widetilde{y})$ and are given by

$$\mu_{LN}(t) = \ln\left[\frac{\mu(t)}{1+\left[\sigma_{SD}(t)/\mu(t)\right]^2}\right] \qquad \text{and} \qquad \left[\sigma_{LN}(t)\right]^2 = \ln\left[1+\left(\frac{\sigma_{SD}(t)}{\mu(t)}\right)^2\right] \tag{3.14}$$

and the error function is defined as

$$\operatorname{erf}\left[Z(t)\right] = \frac{1}{\sqrt{\pi}}\int_{-Z(t)}^{Z(t)}\exp\left(-Y^2\right)\,dY \tag{3.15}$$

$$\left.\begin{array}{c}\text{Gauss PDF} \implies \\ \widetilde{\phi}_G\left[\widetilde{y};\mu(t),\sigma_{ST}(t)\right]\end{array}\right\} = \frac{1}{\sqrt{2\pi}\sigma_{ST}(t)}\exp\left(-\left[\frac{\widetilde{y}-\mu(t)}{\sqrt{2}\sigma_{ST}(t)}\right]^2\right) \qquad \widetilde{y}\in[-\infty,\,\infty] \tag{3.16}$$

$$\left.\begin{array}{c}\text{Gauss CDF} \implies \\ Pr_G\left[\widetilde{y};\mu(t),\sigma_{ST}(t)\right]\end{array}\right\} = \frac{1}{2}\left[1+\text{erf}\left(\frac{\widetilde{y}-\mu(t)}{\sqrt{2}\sigma_{ST}(t)}\right)\right] \qquad \widetilde{y}\in[-\infty,\,\infty] \tag{3.17}$$

$$\left.\begin{array}{c}\text{beta PDF} \implies \\ \widetilde{\phi}_B\left[\widetilde{y};\alpha(t),\beta(t)\right]\end{array}\right\} = \begin{cases}\dfrac{1}{B\left[\alpha(t),\beta(t)\right]}\widetilde{y}^{\alpha(t)-1}(1-\widetilde{y})^{\beta(t)-1} & \widetilde{y}\in\mathbb{R}_{\mathbb{U}} \\ 0 & \widetilde{y}\notin\mathbb{R}_{\mathbb{U}}\end{cases} \tag{3.18}$$

$$\left.\begin{array}{c}\text{beta CDF} \implies \\ Pr_B\left[\widetilde{y};\alpha(t),\beta(t)\right]\end{array}\right\} = \begin{cases}\underbrace{\displaystyle\int_0^{\widetilde{y}} Y^{\alpha(t)-1}(1-Y)^{\beta(t)-1}\,dY}_{\text{incomplete beta function for }\widetilde{y}\in\mathbb{R}_{\mathbb{U}}} & \widetilde{y}\in\mathbb{R}_{\mathbb{U}} \\ 0 & \widetilde{y}\notin\mathbb{R}_{\mathbb{U}}\end{cases} \tag{3.19}$$

The two beta PDF parameters are constrained by

$$\Re\{\alpha(t)\},\Re\{\beta(t)\} > 0 \qquad \text{and} \qquad \Im\{\alpha(t)\} = \Im\{\beta(t)\} = 0 \tag{3.20}$$

with the other PDF parameters similarly limited to real values. Furthermore, the complete beta function $B(\alpha,\beta)$ is defined as

$$B(\alpha,\beta) = \frac{\Gamma[\alpha(t)]\,\Gamma[\beta(t)]}{\Gamma[\alpha(t)+\beta(t)]} = \int_0^1 Y^{\alpha(t)-1}(1-Y)^{\beta(t)-1}\,dY$$

$$\text{with the complete Gamma function} \quad \Gamma[\alpha(t)] = \int_0^\infty Y^{\alpha(t)-1}\exp(-Y)\,dY \tag{3.21}$$

The beta parameters are related to the statistical moments by

$$\mu(t) = \frac{\alpha(t)}{\alpha(t)+\beta(t)} \qquad \text{and} \qquad \sigma_{SD}(t) = \frac{\alpha(t)\,\beta(t)}{\left[\alpha(t)+\beta(t)\right]^2\left[\alpha(t)+\beta(t)+1\right]} \tag{3.22}$$

The above two relations have three pairs of α and β solutions but two are repeated pairs yielding $\alpha(t)=\beta(t)=0$ for $t\in[0,\,\infty]$.

Note that the formal Weibull range for $\widetilde{X}_W$ is semi-infinite and the $\widetilde{\phi}_W$ is such that $Pr_W(1;k,\lambda) < 1$. The size of the departure from unity depends on the amount of scatter, i.e. the magnitude of the standard deviation σ_{ST}, which directly affects the sizes of the parameters α and β

The actual range extends only approximately for $\widetilde{X}_W/\lambda \approx \in [0,\,30]$ for $k=1$. At this point for all practical purposes the exponential term degrades to a zero value. Similar statements, with distinct

$\widetilde{y}$ values, apply to Gauss, log-normal, etc., PDFs. The normalized beta range is of course $\widetilde{X}_B \in [0, 1]$ regardless of data scatter.

Since the viscoelastic moduli and compliances are time and temperature functions, the PDF parameters must have the generic form $\boldsymbol{k}(t) \equiv \boldsymbol{k}[t;T(t)]$, with $\boldsymbol{k}(t)$ formally representing the set of parameters in Eqs. (3.9) – (3.19). Also see Eqs. (3.52). Under more complicated and additional spatial field conditions, the material may be nonhomogeneous and/or temperatures may also become position-dependent and then the parameters become more inclusive as $\boldsymbol{k}(x,t) \equiv \boldsymbol{k}[x,t;T(x,t)]$.

See also Section 8.3 particularly for further treatment of log-normal and beta PDFs.

3.1.3 *Comparison simulations of PDF models*

With all four PDFs having identical mean and standard deviations based on the same preselected[9] set of beta mean $\mu = 0.5043$ and standard deviation $\sigma_{SD} = 0.2838$ values,[10] the various parameters for the Weibull, Gauss, log-normal and beta distributions are computed and compared. The PDFs and associated probabilities were generated in [50] and displayed here in Figs. 1 and 2.

It should be noted from these figures that the various PDFs produce significantly distinct curves for both PDFs and probabilities of occurrence (Pr), i.e. the cumulative distribution functions (CDF). Furthermore PDF values, except for the beta PDF, also exhibit marked differences from the statistical values at $\widetilde{y} = 0$ and $\widetilde{y} = 1$.

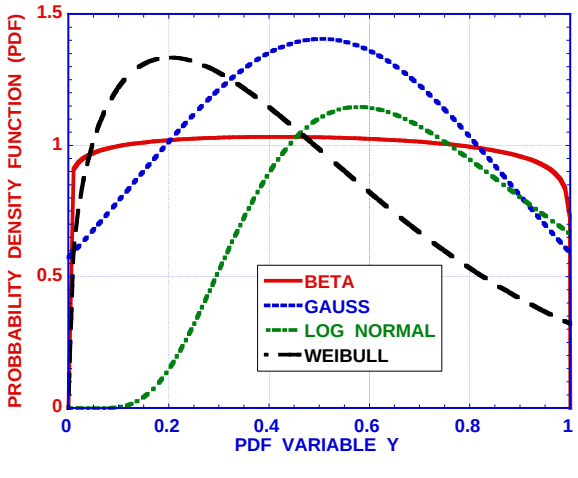

Fig. 1 Probability density functions (PDF) for fitted data with $\alpha = 1.0609$, $\beta = 1.0428$, $\mu = 0.5043$ and $\sigma_{SD} = 0.2838$ [50]

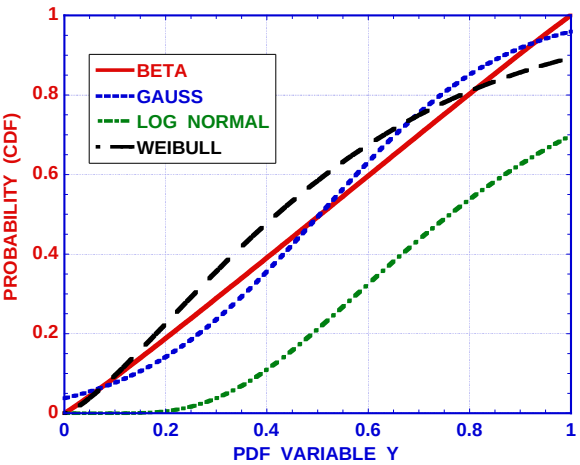

Fig. 2 Probability functions (Pr) or cumulative distribution functions (CDF) [50]

Using the graphs of Fig. 2, the results displayed in Fig. 3 have been constructed using the expression

[9] Corresponding to dynamic E^0 experimental data. See Section 6.

[10] Based on beta distribution values $\alpha = 1.0609$ and $\beta = 1.0428$ which are derived from actual test results. The corresponding Weibull parameters are $k = 1.350$ and $\lambda = 0.5501$ with the log normal values as $\mu_{LN} = -0.2731$ and $\sigma_{SD}^{LN} = 0.5245$. A more extensive treatment is presented in [50].

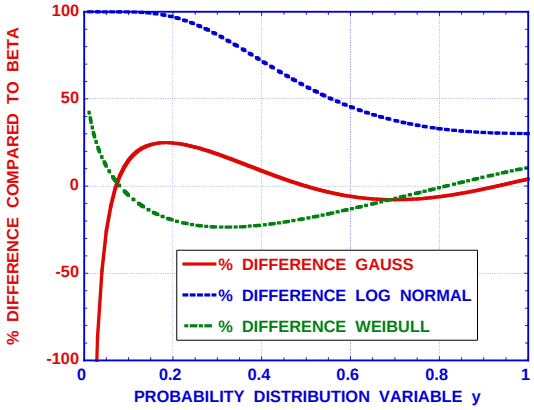

Fig. 3 Percent difference compared to beta probability (CDF) [50]

$$\%\, Pr_{diff}(\widetilde{y}) \;=\; \frac{Pr^{beta}(\widetilde{y}) - Pr^{other}(\widetilde{y})}{Pr^{beta}(\widetilde{y})} \otimes 100\% \tag{3.23}$$

While the PDF differences are large the probability (CDF) dissimilarity values are smaller, except for the region $0 \le \widetilde{y} \le 0.1$. However, they remain significant, largely due to the inability of these PDFs to meet the finite interval $0 \le \widetilde{y} \le 1$ requirements at both or either interval end. These simulations are, of course, influenced by the particular values of the selected mean and standard deviation, however the values chosen here represent typical viscoelastic material property scatter conditions.

Also see Section 7 for statistical analyses pertaining to a vinyl ester resin.

3.2 Linear deterministic viscoelastic media

Consider a Cartesian coordinate system $x = \{x_1, x_2, x_3\}$ with the fully operational Einstein tensor notation. The generalized linear isothermal deterministic constitutive relations have been well established for decades. The characterization is either in terms of relaxation moduli $E_{ijkl}(x,t)$ or creep compliances $C_{ijkl}(x,t)$, such that

$$\sigma_{ij}(x,t) \;=\; \int_{-\infty}^{t} E_{ijkl}(x,t-t') \frac{\partial \varepsilon_{kl}(x,t')}{\partial t'}\, dt' \;=\; E^{0}_{ijkl}(x)\, \varepsilon_{kl}(x,t) \;-\; \int_{0}^{t} \frac{\partial E_{ijkl}(x,t-t')}{\partial t'}\, \varepsilon_{kl}(x,t')\, dt' \tag{3.24}$$

$$\varepsilon_{ij}(x,t) \;=\; \int_{-\infty}^{t} C_{ijkl}(x,t-t') \frac{\partial \sigma_{kl}(x,t')}{\partial t'}\, dt' \;=\; C^{0}_{ijkl}(x)\, \sigma_{kl}(x,t) \;+\; \int_{0}^{t} \frac{\partial C_{ijkl}(x,t-t')}{\partial t'}\, \sigma_{kl}(x,t')\, dt' \tag{3.25}$$

with all state variables at rest at $t = -\infty$. It is to be noted that the characterization process is entirely carried out in real time t rather than in an integral transform space and totally absent of viscoelastic Poisson's ratios [76].

For a uniform spatial load in isotropic and orthotropic isothermal viscoelastic materials Eqs. (3.24) expand into the form

$$\sigma_{11}(t) \;=\; \int_{-\infty}^{t} \left\{ E_{1111}(t-t') \frac{\partial \varepsilon_{11}(t')}{\partial t'} \;+\; E_{1122}(t-t') \frac{\partial \varepsilon_{22}(t')}{\partial t'} \;+\; E_{1133}(t-t') \frac{\partial \varepsilon_{3}(t')}{\partial t'} \right\} dt' \tag{3.26}$$

with two more similar relations. Additionally, isotropic volume changes are governed by

$$\sigma(t) \;=\; \frac{\sigma_{ii}(t)}{3} \;=\; \int\limits_{-\infty}^{t} K(t-t')\frac{\partial \varepsilon(t')}{\partial t'}\,dt' \;=\; \int\limits_{-\infty}^{t} K(t-t')\frac{\partial \varepsilon_{ii}(t')}{3\,\partial t'}\,dt' \tag{3.27}$$

with shape and 1–D length changes described by

$$\sigma_{ij}(t) \;=\; 2\int\limits_{-\infty}^{\infty t} G(t-t')\frac{\partial \varepsilon_{ij}(t')}{\partial t'}\,dt' \quad \text{for} \quad i \neq j \quad \text{and} \quad \sigma_{11}(t) \;=\; \int\limits_{-\infty}^{t} E(t-t')\frac{\varepsilon_{11}(t')}{\partial t'}\,dt' \tag{3.28}$$

accompanied finally by

$$3E_{\underline{iiii}}(t) \;=\; 4G(t)+K(t) \qquad \text{and} \qquad 3E_{\underline{iijj}}(t) \;=\; -2G(t)+K(t) \quad \text{with} \quad i \neq j \tag{3.29}$$

with similar expressions involving compliances.

The isothermal material properties are interrelated through integral transforms, such as Laplace or Fourier (FT), to yield for the latter

$$\imath\,\omega\overline{\overline{E}}(x,\omega) \;=\; \frac{1}{\imath\,\omega\overline{\overline{C}}(x,\omega)} \quad \text{or} \int\limits_{-\infty}^{t} C(x,t-t')\,E(x,t')\,dt' \;=\; \int\limits_{-\infty}^{t} C(x,t)\,E(x,t-t')\,dt' \;=\; t \tag{3.30}$$

since

$$\overline{\overline{\sigma}}_{11}(x,\omega) \;=\; \imath\,\omega\overline{\overline{E}}(x,\omega)\,\overline{\overline{\varepsilon}}_{11}(x,\omega) \qquad \text{and} \qquad \overline{\overline{\varepsilon}}_{11}(x,\omega) \;=\; \imath\,\omega\overline{\overline{C}}(x,\omega)\,\overline{\overline{\sigma}}_{11}(x,\omega)$$
$$\sigma_{11}(x,t) \;\neq\; 0 \;\text{ with all other }\; \sigma_{ij}(x,t) \;=\; 0 \tag{3.31}$$

which are the 1–D isotropic forms of

$$\overline{\overline{\sigma}}_{ij}(x,\omega) \;=\; \imath\,\omega\overline{\overline{E}}_{ijkl}(x,\omega)\,\overline{\overline{\varepsilon}}_{kl}(x,\omega) \qquad \text{and} \qquad \overline{\overline{\varepsilon}}_{ij}(x,\omega) \;=\; \imath\,\omega\overline{\overline{C}}_{ijkl}(x,\omega)\,\overline{\overline{\sigma}}_{kl}(x,\omega) \tag{3.32}$$

While moduli other than Young's obey the inequality

$$\imath\,\omega\overline{\overline{E}}_{ijkl}(x,\omega) \;\neq\; \frac{1}{\imath\,\omega\overline{\overline{C}}_{ijkl}(x,\omega)} \tag{3.33}$$

their matrix identity is

$$\imath\,\omega\left[\overline{\overline{\widehat{E}}}_{ijkl}(x,\omega)\right] \;=\; \frac{1}{\imath\,\omega}\left[\overline{\overline{\widehat{C}}}_{ijkl}(x,\omega)\right]^{-1} \tag{3.34}$$

with the one variable FT defined by

$$\mathscr{F}\left\{\sigma_{ij}(x,t)\right\}(\omega) \;=\; \overline{\overline{\sigma}}_{ij}(x,\omega) \;=\; \int\limits_{-\infty}^{\infty} \sigma_{ij}(x,t)\,\exp\left(-\imath\,\omega t\right)\,dt \tag{3.35}$$

The detailed anisotropic isothermal nonhomogeneous linear viscoelastic material behavior, as exemplified by Fig. 4, is generally represented by Prony series expressions [77], to whit

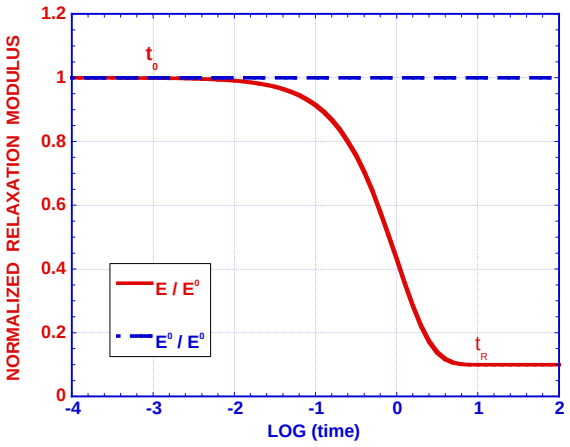

Fig. 4 Typical normalized linear deterministic elastic and viscoelastic moduli

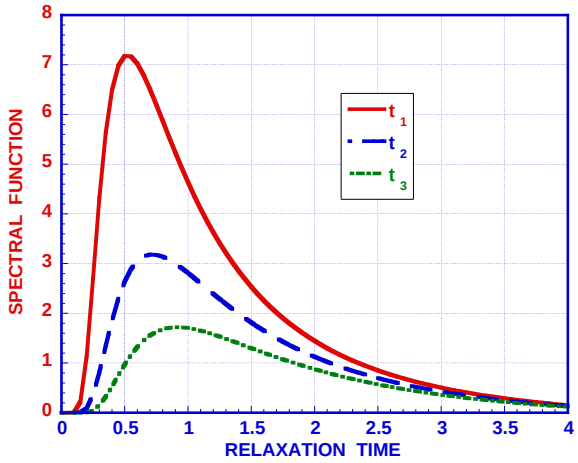

Fig. 5 Deterministic spectral function $E^{s\tau}(\tau,t)$ traces with $t_1 < t_2 < t_3$ & $0 < \tau_R \ll \infty$, (3.39)

$$E_{ijkl}(x,t) \;=\; E^{\infty}_{ijkl}(x) \;+\; \sum_{n=1}^{N_{ijkl}} E_{ijkln}(x) \exp\left(\frac{-\,t}{\tau_{ijkln}(x)}\right) \tag{3.36}$$

with

$$E_{ijkl}(x,0) \;=\; \underbrace{E^{0}_{ijkl}(x)}_{\substack{\text{instantaneous}\\ \text{elastic modulus}}} \;=\; E^{\infty}_{ijkl}(x) \;+\; \sum_{n=1}^{N_{ijkl}} E_{ijkln}(x) \tag{3.37}$$

$$C_{ijkl}(x,0) \;=\; C^{0}_{ijkl}(x) \;=\; C^{\infty}_{ijkl}(x) \;-\; \sum_{n=1}^{N_{ijkl}} C_{ijkln}(x) \tag{3.38}$$

The main reason for this series' popularity and widespread use is its ability to match experimental data admirably. For what appears to be the worst case scenario in the form of complicated high polymers, upper end values of N_{ijkl} are in the range from 10 to 30.

The detailed evaluation of the Prony series coefficients E_{ijkln}, the relaxation times τ_{ijkln} and the number N_{ijkl} of series terms necessary to reach a prescribed accuracy of fit is covered in Section 6.1.

3.3 Material characterization by spectral analysis

The use of spectral representations to model linear time-dependent behavior has been in existence since the late nineteenth century [78], followed by applications and discussions relating to spectral methods by [15] and [63 – 72], to mention a few. In general, a distribution function is selected to represent a generalization of the distribution inherent in a natural system. However, literature surveys reveal that distribution functions were adopted more for their mathematical simplicity rather than their ability to describe realistic viscoelastic behavior. For example, a "box function" or step function was used either singly or in combination with a "wedge" or power law distribution function [25]. The selected spectral function is then used to develop viscoelastic material functions using the elastic-viscoelastic correspondence principle (EVCP), based on Laplace and/or Fourier transforms.

Subsequently upon inversion to real time, one can obtain the material response. In the following discussion, a spectral function is selected based on certain criteria that mimic the response of natural systems. The spectral function must satisfy criteria of being non-negative, bounded, monotonic and able to produce constant values in defined regions. An extended derivation and discussion of the spectral method can be found in [67 – 70] and for completeness, a brief overview is presented next.

For simplicity's sake[11] let the viscoelastic Young's modulus $E(x,t)$ Prony series of (3.36) be reformulated to contain an infinite number of relaxation times with $N \to \infty$. Then for a continuous spectrum of relaxation times

$$E(x,t) \;=\; \lim_{N\to\infty}\left\{\sum_{n=1}^{N} E_n(x)\exp\left(\frac{-t}{\tau_n(x)}\right)\right\} \;\to$$

$$\int_0^\infty \underbrace{E^{\tau}(x,\tau)\exp\left(\frac{-t}{\tau}\right)}_{=\,E^{s\tau}(\tau;x,t)}\,d\tau \;=\; \int_0^\infty \underbrace{\frac{E^{*\tau}(x,\tau^*)}{\tau^*}\exp\left(-t\,\tau^*\right)}_{=\,E^{*s\tau}(\tau^*;x,t)}\,d\tau^* \;=\; E^{sp}(x,t) \tag{3.39}$$

for $\tau = 1/\tau^*$. The second integral is, of course, the LT of the integrand without the exponential function. This expression can be readily extended to TSMs by substituting $t = \xi$ and to all deterministic and stochastic moduli and compliances by introducing the appropriate PDF. See Section 3.5.

Spectral functions $E^{s\tau}(\tau;x,t)$ must satisfy the criteria of being non-negative, bounded, monotonic and be able to vanish at prescribed relaxation times. Therefore, they should satisfy the following conditions

$$E^{s\tau}(0;x) \;=\; E^{s\tau}(\tau_R;x) \;=\; 0,\;\; E^{s\tau}(\tau,x) \;=\; 0 \;\; \tau\in[-\infty,\,0] \;\;\&\;\; \in[\tau_R,\,\infty],$$

$$E^{s\tau}(\tau;x) \;\geq\; 0 \quad \tau\in[0,\,\infty] \tag{3.40}$$

with $\tau_R \ll \infty$. Typical spectral function shapes of $E^{s\tau}(\tau;x_a,t)$ at some combined spatial position $x_a = \{x_{1a},x_{2a},x_{3a}\}$ and at several times t are shown in Fig. 5. A 3–D surface plot of $E^{\tau}(\tau;x,t)$ vs. τ and t would show its decay in real time as exemplified by the traces in the E vs. t space of Fig. 4. The matching of the spectral functions to experimental data through LSQ protocols [79] is described in Section 6.1.3.

The constitutive relations with isothermal spectral moduli then are in the form

$$\sigma_{ij}(x,t) \;=\; \int_{-\infty}^{t} \underbrace{\left\{\int_0^\infty \overbrace{E^{\tau}_{ijkl}(\tau;x)\exp\left(\frac{-t'}{\tau}\right)}^{=\,E^{s\tau}(\tau;x,t)}\,d\tau\right\}}_{=\,E^{sp}_{ijkl}(x,t')} \frac{\partial\varepsilon_{kl}(x,t-t')}{\partial t'}\,dt' \;= \tag{3.41a}$$

$$\int_{-\infty}^{t}\frac{\partial}{\partial t'}\left\{\int_0^\infty E^{\tau}_{ijkl}(\tau;x)\exp\left(\frac{-t'}{\tau}\right)d\tau\right\}\varepsilon_{kl}(x,t-t')\,dt' \;= \tag{3.41b}$$

$$-\int_{-\infty}^{t}\left\{\int_0^\infty E^{\tau}_{ijkl}(\tau;x)\exp\left(\frac{-t'}{\tau}\right)\frac{d\tau}{\tau}\right\}\varepsilon_{kl}(x,t-t')\,dt' \;= \tag{3.41c}$$

[11] The same procedure is applicable to all moduli $E_{ijkl}(x,t)$ and compliances $C_{ijkl}(x,t)$.

$$-\int_{-\infty}^{t}\underbrace{\left\{\int_{0}^{\infty}E^{*\tau}_{ijkl}(\tau^*;x)\exp\left(-\tau^* t'\right)\,d\tau^*\right\}}_{=E^{*sp}_{ijkl}(x,t')}\varepsilon_{kl}(x,t-t')\,dt' \tag{3.41d}$$

with Fourier transforms

$$\bar{\bar{\sigma}}_{ij}(x,\omega)\;=\;\imath\,\omega\,\bar{\bar{E}}^{sp}_{ijkl}(x,\omega)\,\bar{\bar{\varepsilon}}_{kl}(x,\omega)\quad\text{or}\quad\bar{\bar{\sigma}}^{*}_{ij}(x,\omega^*)\;=\;\bar{\bar{E}}^{*sp}_{ijkl}(x,\omega^*)\,\bar{\bar{\varepsilon}}_{kl}(x,\omega^*) \tag{3.42}$$

This relation has the same form as the Prony series representation since there is a unique time function $E_{ijkl}(x,t)$ set for each material that can be characterized in a number of equivalent arrangements.

The identification of the second integral in (3.39) as the LT of $E^*(x,\tau^*)=E^{*\tau}(x,\tau^*)/\tau^*$ significantly eases the analytic evaluation of this integral. For instance, for complicated functions it can be determined by Post's formula [80] to yield

$$E^{sp}(x,t)\;=\;\lim_{k\to\infty}\left\{\frac{(-1)^k}{k!}\left(\frac{k}{t}\right)^{k+1}\frac{d^kE^*(x,\tau^*)}{d\tau^{*k}}\bigg|_{\tau^*=k/t}\right\} \tag{3.43}$$

The expression formally converges for $k\to\infty$ and is approximate for $k<\infty$. However, reasonable numerical convergence can be expected with a limited number of terms. The differentiations can be carried out symbolically by such software as MAPLE,™ MATHEMATICA,™ MATLAB,™ etc.

Furthermore, the relation between the bilateral LT and the FT defined by (3.35) is

$$\mathscr{BL}\left\{F(t)\right\}(s)\;=\;\int_{-\infty}^{\infty}F(t)\exp(-st)\,dt\;=\;\mathscr{L}\left\{F(t)\right\}(s)+\mathscr{L}\left\{F(-t)\right\}(-s)\;=$$

$$\mathscr{F}\left\{F(t)\right\}(\omega)\Big|_{\imath\omega=s}\;=\;\bar{\bar{F}}(\omega)\Big|_{\imath\omega=s} \tag{3.44}$$

indicating that the Post relation (3.43) can be used for FTs as well as LTs. This is particularly true if the starting conditions are properly stated – particularly at $t=0-$ as

$$\sigma_{ij}(x,t)\;=\;\varepsilon_{ij}(x,t)\;=\;u_i(x,t)\;=\;0\qquad t\in[-\infty,\,0] \tag{3.45}$$

Under these ICs, the bilateral LT reduces to the ordinary LT in the semi infinite space $t\in[0,\,\infty]$ and to the half interval FT in the positive half infinite space. See also Section 5.2.

3.4 Material characterization by fractional derivatives (FDs)

Other possible constitutive relation characterizations are through fractional, rather than integer, time derivatives and integrals[12] [81 – 89]. The concept has been generalized in Ref. [85] by extending it to linear anisotropic viscoelasticity and by the addition of a series of FDs with multiple parameters in order to more broadly represent FD moduli and compliances.

Two utilitarian forms present themselves, namely the Riemann-Liouville (RL) and Caputo (Ca) forms. While their introduction alters the detailed viscoelastic expressions for moduli and compliances, it preserves all analytical, experimental, deterministic and probabilistic protocols for pertinent parameter determinations as formulated herein.

[12] For extensive bibliographies see [83 – 86].

In order to develop the FD constitutive relations consider a 1–D loading represented by (3.28). Let the generic n-th FD be designated by $D_n^{\alpha_n}(t;\alpha_n)$. Then the stress-strain relation for the n-th single Kelvin model with a non-Newtonian FD dashpot and an elastic spring in parallel is

$$D_n^{\alpha_n}\left\{\varepsilon_{11}^{(n)}(x,t)\right\} + \frac{\varepsilon_{11}^{(n)}(x,t)}{\tau_n(x)} = \frac{\sigma_{11}(x,t)}{\eta_n} \tag{3.46}$$

Since a general analytical solution to (3.46) is unavailable, the formulation of the general Kelvin model (GKM) will take place in the FT space, to whit

$$\overline{\overline{D_n^{\alpha_n}\{\varepsilon_{11}^{(n)}(x,\omega)\}}} + E^{(n)}(x)\,\overline{\overline{\varepsilon_{kl}^{(n)}}}(x,\omega) = \overline{\overline{\sigma_{11}}}(x,\omega) = \overline{\overline{E_n^*}}(x,\omega;\alpha_n)\,\overline{\overline{\varepsilon_{11}^{(n)}}}(x,\omega) \tag{3.47}$$

where $E^{(n)}$ is the spring constant (modulus) and E_n^* the modulus for the single KMs. The modulus E_n^{FD} emerges since the FD operators $D_n^{\alpha_n}$ generally are convolution integrals.

Then for the GKM one only needs to sum the contributions of the N individual KMs in series with each other and a single elastic spring

$$\begin{aligned}\bar{\bar{\sigma}}_{11}(x,\omega) &= \left(E^0(x) + \left[\sum_{n=1}^{N}\left\{\frac{1}{\overline{\overline{E_n^*}}(x,\omega;\alpha_n)}\right\}\right]^{-1}\right)\bar{\bar{\varepsilon}}_{11}(x,\omega)\\ &= \left(E^0(x) + \overline{\overline{E_n^{FD}}}(x,\omega;\alpha_n)\right)\bar{\bar{\varepsilon}}_{11}(x,\omega)\end{aligned} \tag{3.48}$$

The contributions from the two FDs $D_{\underline{ijkln}}^{\alpha_{ijkln}}(x,t;\alpha_{\underline{ijkln}})$ to anisotropic constitutive relations are [85]

$$\text{RL} \implies \sigma_{ij}(x,t) = \sum_{n=1}^{N_{\underline{ijkl}}^{RL}}\sum_{k,l=1}^{3} D_{\underline{ijkln}}^{RL\alpha_{\underline{ijkln}}}\{\varepsilon_{kl}(x,t)\} =$$

$$\sum_{n=1}^{N_{\underline{ijkl}}^{RL}}\sum_{k,l=1}^{3}\frac{E_{\underline{ijkln}}^{FDRL}(x)}{\Gamma[n-\alpha_{\underline{ijkln}}(x)]}\frac{\partial^n}{\partial t^n}\left\{\int_0^t \frac{\varepsilon_{kl}(x,t')\,dt'}{\left[(t-t')/\tau_{\underline{ijkln}}^{FDRL}(x)\right]^{\alpha_{\underline{ijkln}}+1-n}}\right\} \quad \text{with } n-1<\alpha_{ijkln}<n \tag{3.49}$$

$$\text{Ca} \implies \sigma_{ij}(x,t) = \sum_{n=1}^{N_{\underline{ijkl}}^{Ca}}\sum_{k,l=1}^{3} D_{\underline{ijkln}}^{Ca\alpha_{\underline{ijkln}}}\{\varepsilon_{kl}(x,t)\} =$$

$$\sum_{n=1}^{N_{\underline{ijkl}}^{Ca}}\sum_{k,l=1}^{3}\frac{E_{\underline{ijkln}}^{FDCa}(x)}{\Gamma[n-\alpha_{\underline{ijkln}}(x)]}\int_0^t \frac{\partial^n\varepsilon_{kl}(x,t')}{\partial t'^n}\frac{dt'}{\left[(t-t')/\tau_{\underline{ijkln}}^{FDCa}(x)\right]^{\alpha_{\underline{ijkln}}(x)+1-n}} \tag{3.50}$$

with the same constraints on the α_{ijkln} as noted in (3.49). In both cases when $\alpha_{ijkln}=n$ then the fractional derivatives reduce to integer order derivatives. It is self evident that a similar FD construction can be constructed for anisotropic compliances $C_{ijkl}(x,t)$.

The repeated differentiation of integrals in (3.49) make the RL FDs much more complicated than the Caputo ones. In general the coefficients $E_{ijkln}^{FDRL} \neq E_{ijkln}^{FDCa} \neq E_{ijkl}$, but for sufficiently large N_{ijkl}s the two modulus expressions should yield approximately equal values with similar results for Prony series and spectral representations. Both FD expressions are subject to the constraints

$$t' \le t \in [0,\,\infty]; \qquad \alpha_{ijkln} > 0; \qquad \alpha_{ijkln} > n-1; \qquad n \in [1,\,N_{ijkl}] \tag{3.51}$$

with each α_{ijkln} not an integer. Also see Section 8.2.

3.5 Linear stochastic media

3.5.1 *A "simple" expression*

Let the generic PDFs $\widetilde{\phi}\,[\widetilde{y};\boldsymbol{k}(t)]$ be identified as

$$\widetilde{\phi}\,[\widetilde{y};\boldsymbol{k}(t)] \;=\; \begin{cases} \widetilde{\phi}_W\,[\widetilde{y};\boldsymbol{k_W}(t)] \;=\; \widetilde{\phi}_W\,[\widetilde{y};k(t),\lambda(t)] & \text{Weibull} \\ \widetilde{\phi}_{LN}\,[\widetilde{y};\boldsymbol{k_{LN}}(t)] \;=\; \widetilde{\phi}_{LN}\,[\widetilde{y};\mu(t),\sigma_{ST}(t)] & \log-\text{normal} \\ \widetilde{\phi}_G\,[\widetilde{y};\boldsymbol{k_G}(t)] \;=\; \widetilde{\phi}_G\,[\widetilde{y};\mu(t),\sigma_{ST}(t)] & \text{Gauss} \\ \widetilde{\phi}_B\,[\widetilde{y};\boldsymbol{k_B}(t)] \;=\; \widetilde{\phi}_B\,[\widetilde{y};\alpha(t),\beta(t)] & \text{beta} \end{cases} \tag{3.52}$$

with $\boldsymbol{k}(t) \equiv \boldsymbol{k}\,[t;T(t)]$, or more generally $\boldsymbol{k}(t) \equiv\equiv \boldsymbol{k}(x,t) \equiv \boldsymbol{k}\,[x,t;T(x,t)]$, as the set of parameters specific to each selected PDF and with similar expressions for other PDFs. Also see Eqs. (3.9) – (3.19).

A possible and plausible stochastic modulus and compliance representation is to simply multiply their deterministic expression by a chosen PDF, such that

$$\text{Formulation A}: \quad \underbrace{\widetilde{E}_{ijkl}\left(x,t;\widetilde{\phi}\,[\widetilde{y};\boldsymbol{k}(t)]\right)}_{\text{stochastic modulus}} \;=\; \underbrace{\widetilde{\phi}\,[\widetilde{y};\boldsymbol{k}(t)]}_{\substack{\text{stochastic}\\ \text{function}}}\;\underbrace{E_{ijkl}(x,t)}_{\substack{\text{deterministic}\\ \text{modulus}}} \tag{3.53}$$

with similar expressions for shear and bulk moduli and for compliances.

Consequently the random isothermal constitutive relations now become

$$\widetilde{\sigma}_{ij}\left(x,t;\widetilde{\phi}^{\sigma}\,[\widetilde{y};\boldsymbol{k}(t)]\right) \;=\; \int_{-\infty}^{t} \underbrace{\widetilde{E}_{ijkl}\left(x,t-t';\widetilde{\phi}\,[\widetilde{y};\boldsymbol{k}(t-t')]\right)}_{=\,\widetilde{E}_{ijkl}(x,t,t')} \frac{\partial\widetilde{\varepsilon}_{kl}\left(x,t';\widetilde{\phi}^{\varepsilon}\,[\widetilde{y};\boldsymbol{k}(t')]\right)}{\partial t'}\,dt' \tag{3.54}$$

and

$$\widetilde{\varepsilon}_{ij}\left(x,t;\widetilde{\phi}^{\varepsilon}\,[\widetilde{y};\boldsymbol{k}(t)]\right) \;=\; \int_{-\infty}^{t} \underbrace{\widetilde{C}_{ijkl}\left(x,t-t';\widetilde{\phi}^{C}\,[\widetilde{y};\boldsymbol{k}(t-t')]\right)}_{=\,\widetilde{C}_{ijkl}(x,t,t')} \frac{\partial\widetilde{\sigma}_{kl}\left(x,t';\widetilde{\phi}^{\sigma}\,[\widetilde{y};\boldsymbol{k}(t')]\right)}{\partial t'}\,dt' \tag{3.55}$$

For variable $T(x,t')$ all convolution functions depending on $t-t'$ change to t,t'.

3.5.2 *Two more inclusive but very complicated stochastic modulus/compliance expressions*

In alternate and more general stochastic modulus and compliance constructions one can assign randomness to individual Kelvin models or to to each and every coefficient and relaxation time of Eqs. (3.36), such that

$$\text{Formulation B}: \quad \widetilde{E}_{ijkl}\left(x,t;\widetilde{\phi}\,[\widetilde{y};\boldsymbol{k}(t)]\right) \;=$$

$$\phi_{\infty}\!\left(\widetilde{\phi}_{\infty}\,[\widetilde{y};\boldsymbol{k}(t)]\right)\widetilde{E}^{\infty}_{ijkl}(x) \;+\; \sum_{n=1}^{N_{ijkl}} \widetilde{\phi}_{n1}\,[\widetilde{y};\boldsymbol{k}(t)]\,\underline{E_{ijkln}}(x)\exp\left(\frac{-\,t}{\widetilde{\phi}_{n2}\,[\widetilde{y};\boldsymbol{k}(t)]\,\underline{\tau_{ijkln}}(x)}\right) \tag{3.56}$$

and

$$\text{Formulation C}: \ \widetilde{E}_{ijkl}\left(x,t;\widetilde{\phi}\left[\widetilde{y};\boldsymbol{k}(t)\right]\right) =$$

$$\widetilde{E}^{\infty}_{ijkl}\left(x;\widetilde{\phi}_{\infty 3}\left[\widetilde{y};\boldsymbol{k}(t)\right]\right) + \sum_{n=1}^{N_{ijkl}} \widetilde{E}_{\underline{ijkl}n}\left(x;\widetilde{\phi}_{n4}\left[\widetilde{y};\boldsymbol{k}(t)\right]\right) \exp\left(\frac{-t}{\tau_{\underline{ijkl}n}\left[x;\widetilde{\phi}_{n5}\left[\widetilde{y};\boldsymbol{k}(t)\right]\right]}\right) \tag{3.57}$$

and similar expressions for compliances.

The Formulation C random constitutive relations have their origin in the generalized Kelvin model (GKM) where every spring and damper is assigned separate stochastic properties. While this approach embodies the most precise high fidelity approach to viscoelastic probabilistic characterization analysis, its use, at the moment, is nevertheless impractical for eventual engineering stress analysis due to the scarcity of random viscoelastic measured data, its high mathematical complexity and due to its relative CPU intensive computational demands.

It must be noted that the stochastic expressions (3.56) and (3.57) are highly complicated and do not readily lend themselves to analytical viscoelastic solutions. The much simpler ones of Eqs. (3.54) and (3.55) do not offer any more hope for obtaining analytical solutions, but are less computationally intensive. None of the three probabilistic formulations offer analytical LTs or FTs since their complicated mathematical expressions lead to integrals that can be evaluated in an analytical format.

4 ANALYSIS II: VARIABLE TEMPERATURE CONDITIONS

4.1 Deterministic thermorheologically simple materials (TSM)

It is a well documented fact that viscoelastic material properties are extremely sensitive to temperature variations [90 – 92]. These manifestations come in the form of changes in the principal coefficient of viscosity of roughly one order of magnitude for every 20℃.

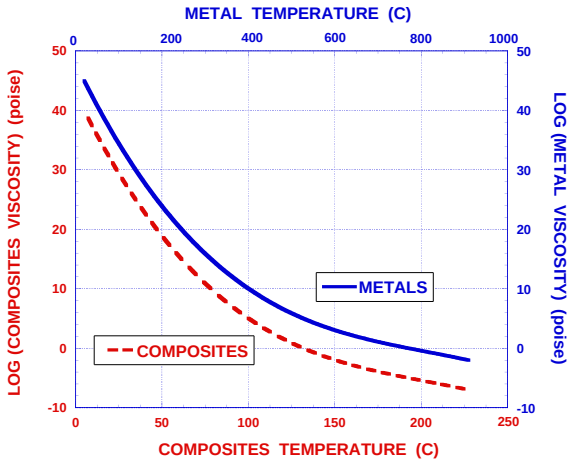

Fig. 6 Viscosity–temperature evolution

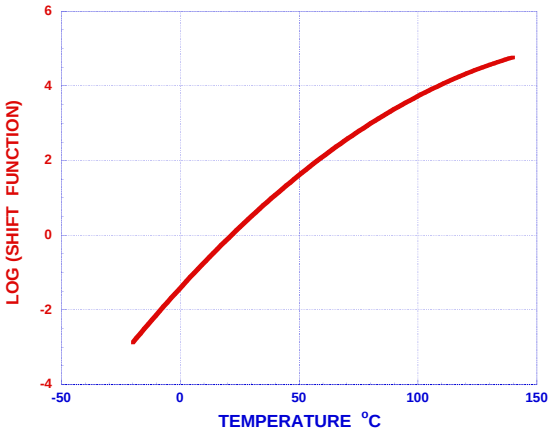

Fig. 7 Shift factor a_T with increasing temperatures

It has been further demonstrated that for thermorheologically simple materials (TSMs) this dependency can be codified in a WLF shift factor[13] $a(T)$ and a reduced or pseudo time $\xi(x,t)$ defined by [90 – 92]

$$\log\left[a_T(T)\right] \;=\; \frac{-\widehat{C}_1(T-T_r)}{\widehat{C}_2+T-T_r} \tag{4.1}$$

$$\xi\left[x,t;a_T(T)\right] \;=\; \int_0^t a_T\left[T(x,t')\right]\,dt' \tag{4.2}$$

where T_r is a reference temperature where $a_T(T_r)=1$, i.e. no time–temperature shift, and $\xi(T_r)=t$.

While this transformation restores the convolution integral concept in the ξ space as

$$\sigma_{ij}(x,t) \;=\; \widehat{\sigma}_{ij}\left[x,\xi(x,t)\right] \;=\; \int_{-\infty}^{\xi(x,t)} \widehat{E}_{ijkl}\left[\xi(x,t)-\xi'\right]\frac{\partial\widehat{\varepsilon}_{kl}(x,\xi')}{\partial\xi'}\,d\xi' \tag{4.3}$$

and produces a master relaxation modulus $\widehat{E}_{ijkl}(x,t)$ it nevertheless destroys the relative simplicity of the constant coefficient field equations. Thus even in the relatively simple quasi-static case

$$\frac{\partial\sigma_{ij}(x,t)}{\partial x_j} \;=\; 0 \qquad\Longrightarrow\qquad \frac{\partial\xi(x,t)}{\partial x_m}\,\frac{\partial\widehat{\sigma}_{ik}\left[x,\xi(x,t)\right]}{\partial\xi} \;=\; 0 \tag{4.4}$$

they are turned into PDEs with variable coefficients. Consequently, even for the simplest variable temperature-dependent problem no formal EVCP (analogy) [1 – 22] can be applied unless approximate analogies [93 – 94] are substituted and applied.

4.2 Stochastic thermorheologically simple materials (STSM)

A pertinent portion of stochastic thermo-viscoelasticity is presented in [36] and the differences as well as similarities between deterministic thermo-elasticity and thermo-viscoelasticity are noted in [95]. The primary concern in this publication is in relation to stochastic variable temperature effects on material properties, which can manifest themselves in the following combinations with indicated PDFs associated with Eqs. (4.1) and (4.2)

I – deterministic temperatures and stochastic shift function: $\widetilde{a}_{1T}\left[\widetilde{y};T\left(x,t\right)\right] \;=\; \widetilde{\phi}_1^{a_T}\left[\widetilde{y};T(x,t)\right]a_T\left[T(x,t)\right]$

II – stochastic temperatures and deterministic shift function: $\widetilde{a}_{2T}\left[\widetilde{T}(\widetilde{y};x,t)\right] \;=\; a_T\left[\widetilde{T}(\widetilde{y};x,t)\right]$

III – stochastic temperatures coupled with stochastic shift functions: $\widetilde{a}_{3T}\left[\widetilde{y};\widetilde{T}(\widetilde{y};x,t)\right]$

See Section 3.5.1 for possible stochastic forms of the temperature $\widetilde{T}$ and the shift PDF $\widetilde{a}_T$.

Obviously the uncertainty of the temperature fields or shift functions or both greatly complicates the analysis and its solutions. Additionally, the stochastic reduced time is now replaced by a modified (4.2) as

$$\widetilde{\xi}\left[x,t;\widetilde{a}_T\left(\widetilde{T}(\widetilde{y};x,t)\right)\right] \;=\; \int_0^t \widetilde{a}_T\left[\widetilde{y};\widetilde{T}(\widetilde{y};x,t'')\right]\,dt'' \tag{4.5}$$

and leads to an expression that greatly complicates any analysis. Furthermore, for stochastic or deterministic temperatures which are time-dependent no EVCP or stochastic EVCP (SEVCP) can be formulated.

[13] Also known as the Williams-Landel-Ferry shift function.

4.3 Stochastic isothermal elastic–viscoelastic correspondence principles (SEVCP)

A limited extension of the deterministic EVCP to incompressible stochastic viscoelastic media, i.e. $K(x,t) = \infty$ for $t \in [-\infty, \infty]$, may be found in [51]. This concept can be generalized for Formulation A of (3.53) since Eq. (3.54) can be rewritten as

$$\widetilde{\sigma}_{ij}\left(x,t;\widetilde{\phi}^{\sigma}[\widetilde{y};\boldsymbol{k}(t)]\right) \;=\; \widetilde{\phi}^{\sigma}(\widetilde{y},t)\,\sigma_{ij}(x,t) \;=$$

$$\int_{-\infty}^{t} \widetilde{\phi}\,(\widetilde{y},t-t')\,E_{ijkl}(x,t-t')\,\frac{\partial\left[\widetilde{\phi}^{\varepsilon}(\widetilde{y},t')\,\varepsilon_{kl}(x,t')\right]}{\partial t'}\,dt' \tag{4.6}$$

Taking the FT of (4.6) yields

$$\overline{\overline{\widetilde{\phi}^{\sigma}(\widetilde{y},\omega)\,\sigma_{ij}(x,\omega)}} \;=\; \imath\omega\,\overline{\overline{\widetilde{\phi}\,(\widetilde{y},\omega)\,E_{ijkl}(x,\omega)}}\;\overline{\overline{\widetilde{\phi}^{\varepsilon}(\widetilde{y},t')\,\varepsilon_{kl}(x,t')}} \tag{4.7}$$

which in effect is equivalent to

$$\overline{\overline{\widetilde{\sigma}}}_{ij}(x,\omega;\widetilde{y}) \;=\; \imath\omega\,\overline{\overline{\widetilde{E}}}_{ijkl}(x,\omega;\widetilde{y})\;\overline{\overline{\widetilde{\varepsilon}}}_{kl}(x,\omega;\widetilde{y}) \tag{4.8}$$

Similarly the FT of the three stochastic field equations become

$$\frac{\partial\overline{\overline{\widetilde{\sigma}}}_{ij}(x,\omega;\widetilde{y})}{\partial x_j} + \underbrace{\overline{\overline{\widetilde{f}}}_{i}(x,\omega;\widetilde{y})}_{\substack{\text{random potential}\\ \text{body forces}}} \;=\; \underbrace{\mathscr{F}\left\{\frac{\partial}{\partial t}\left(\widetilde{\rho}\,(x,t;\widetilde{y})\,\frac{\partial\widetilde{u}_i(x,t;\widetilde{y})}{\partial t}\right)\right\}}_{\text{random inertia term}} \;=\; \imath\omega\,\overline{\overline{\widetilde{\rho}\,(x,t;\widetilde{y})\,\frac{\partial\widetilde{u}_i(x,t;\widetilde{y})}{\partial t}}} \tag{4.9}$$

These viscoelastic FT relations are equivalent in form to their elastic FT counterparts, thereby establishing the foundation for the SEVCP. However these expressions are of sufficiently significant complexity to negate any possibility of generating detailed analytic expressions for their FTs and their subsequent inversions. Consequently, the practical utility of the SEVCP approach is at most limited if at all realizable.

The general FT expressions for Formulations B and C are identical except for the inherently more complicated stochastic details. Consequently, their practicality raises the same questions as Formulation A has above.

5 EXPERIMENTAL PROTOCOLS

5.1 General comments

The cardinal rules in combined analytical and experimental material property characterization procedures are the unparalleled demands for (a) the construction of meaningful simple experiments that are (b) amenable to analytical solutions. With this dictum in mind, one is generally limited to 1–D experiments, such as simple tension or compression (without bending if possible) of uniform rectangular coupons, and torsion of solid circular cylinders, all with surface stress and strain measurements. In the tension case, measurements are taken of the applied force ($\rightarrow \sigma_{11}(t) \neq 0, \sigma_{22}(t) = \sigma_{33}(t) = 0$), normal strains in two perpendicular directions[14] ($\varepsilon_{11}(t)$ and $\varepsilon_{22}(t)$) and of time (t). Whereas in the

[14] For 1–D loading conditions and isotropic media $\varepsilon_{22}(t) = \varepsilon_{33}(t)$ with $E_{1122}(t) = E_{1133}(t) = E_{2211}(t)$, etc.

torsion experiments, the applied torque $(\rightarrow \sigma_{12}(t))$, the angular twist $(\theta(t) \rightarrow \varepsilon_{12}(t))$ and time are continuously recorded. It is not uncommon in high polymers that compression moduli exceed by several orders of magnitude their tension counterparts. Indeed, such is the case of the polymeric material whose dynamic 1–D tension responses are displayed in Fig. 11, which shows the evolution in time of the two accelerometer accelerations and of the impact force.

Then in 1–D linear isotropic isothermal viscoelastic media, all isotropic moduli, and conversely all compliances, can be determined from Eqs. (3.26) and (3.29) with

$$\sigma_{11}(t) = \int_{-\infty}^{t} \left\{ E_{1111}(t-t') \frac{\partial \varepsilon_{11}(t')}{\partial t'} + 2E_{1122}(t-t') \frac{\partial \varepsilon_{22}(t')}{\partial t'} \right\} dt' \tag{5.1}$$

$$\sigma_{22}(t) = 0 = \int_{-\infty}^{t} \left\{ E_{1122}(t-t') \frac{\partial \varepsilon_{22}(t')}{\partial t'} + \left[E_{1111}(t-t') + E_{1122}(t-t') \right] \frac{\partial \varepsilon_{22}(t')}{\partial t'} \right\} dt' \tag{5.2}$$

See Section 5.3.

For 1–D displacement/stress wave dynamic experiments, only the stress $\sigma_{11}(x_1,t)$, the accelerations $\dfrac{\partial^2 u_1(x_1,t)}{\partial t^2}$ and time t are needed and measured to determine the instantaneous elastic modulus. See Section 5.4 for details.

5.2 Starting transient loads

Various analyses and experiments have demonstrated the important influence of the starting loads on early and subsequent later viscoelastic material responses [50], [96 – 108]. The inclusion of the starting transients is of particular importance when approaching constant conditions such as relaxation or creep (Fig. 8), where

$$\sigma_{11}(x,t), \varepsilon_{11}(x,t) = \begin{cases} 0 & t \in [-\infty,\ 0] \text{ rest state} \\ \boldsymbol{f_L}(t) = \{f_L^{\sigma}(t), f_L^{\varepsilon}(t)\} & t \in [0,\ t_1] \quad \text{loading cycle} \\ \boldsymbol{const.} = \{\sigma_{11}^{c}(x,t), \varepsilon_{11}^{c}(x,t)\} & t \in [t_1,\ t_2] \quad \text{steady state} \\ \boldsymbol{f_U}(t) = \{f_U^{\sigma}(t), f_U^{\varepsilon}(t)\} & t \in [t_2,\ t_3] \quad \text{unloading cycle} \\ 0 & t \in [t_3, \infty] \quad \text{rest state} \end{cases} \tag{5.3}$$

Once the loading cycle has stabilized at some $t = t_1$, the constant values indicate creep for σ_{11}^{c} and relaxation for ε_{11}^{c}. Note that for the latter state ε_{22} is at least a time function since $E_{1111}(t) \neq E_{1122}(t)$. If these two moduli were equal then according Eq. (3.29) $G(t) = K(t) = E_{1111} = E_{1122} = 0$. On the other hand, the very special case of $E_{1111}(t) = c_0 E_{1122}(t)$ with $G(t) = c_1 K(t)$ with the two c_i equal to constants is a possibility [98].

For continuity requirements to be satisfied, the functions $f^{\sigma}(x,t)$ or $f^{\varepsilon}(x,t)$ must satisfy the following conditions

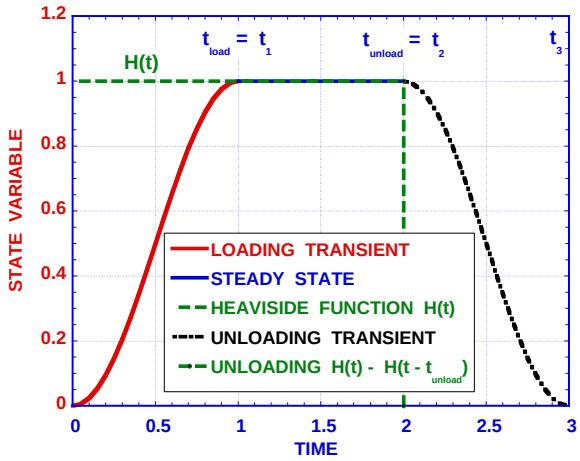

Fig. 8 Schematic of starting transient, steady-state and Heaviside loadings [76]

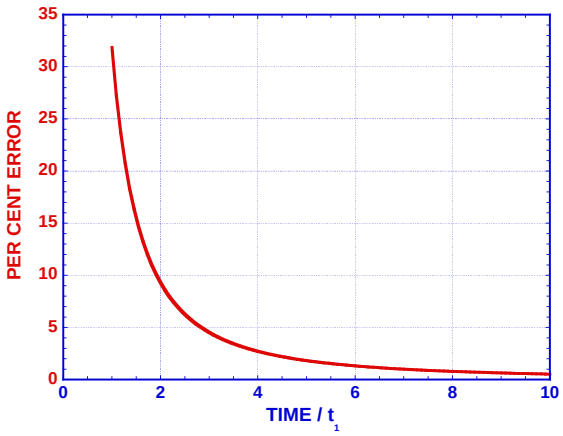

Fig. 9 Error in viscoelastic strains by disregarding starting load transients for data from [96]

$$f(x,t)\Big|_{\substack{t=0\\t=t_3}} = \frac{\partial f(x,t)}{\partial t}\Big|_{t=0,t_1,t_2,t_3} = 0 \quad \text{and} \quad f(x,t)\Big|_{t=t_1,t_2} = const. \tag{5.4}$$

If a controlled unloading process is to take place starting at $t = t_2 > t_1$, then the unloading time function will generally differ from the loading one, i.e. $f_L \neq f_U$.

Fig. 8 is a schematic representation of the Heaviside function and actual loading and unloading cycles. The real time model of gradual load rise and fall and the beginning and terminating zero slopes avoids the infinite accelerations associated with the mathematically correct but physically unattainable Heaviside model. Fig. 9 depicts the resulting errors, particularly at the early times, if the starting load transients are neglected. It should be noted that the time t_1 required to reach constant loading conditions on mechanical test frames can be a significant number of minutes [50], [56 – 62], [99], [102 – 108].

5.3 Linear 1–D quasi-static measurements

Quasi-static data is best acquired in a tension/compression testing machine. The measurements consist of the 1–D load ($\sigma_{11}(t)$) through a load cell, 2–D strains ($\varepsilon_{11}(t)$ and $\sigma_{22}(t)$ by two synchronized high speed cameras and of real time (t). This set of data covers the necessary state variables and is sufficient to generate all moduli in real time by using Eqs. (3.26) to (3.29), (5.1) and (5.2). The pertinent computational protocol are presented in subsequent sections.

5.4 The instantaneous elastic moduli from dynamic wave propagation experiments

5.4.1 *Axial compression or tension stresses and waves*

The illusive instantaneous moduli $\widetilde{E}^0_{ijkl}(\widetilde{y}) = \widetilde{E}_{ijkl}(0;\widetilde{y})$ are difficult to capture from even simple 1–D quasi-static relaxation or creep experiments. The fundamental difficulty stems from the fact that at zero time $\sigma_{ij}(0) = \varepsilon_{ij}(0) = 0$. For instance, even the relatively simple Young's modulus defined as

$$\widetilde{E}^0(\widetilde{y}) \;=\; \lim_{t\to 0}\left[\frac{\partial\widetilde{\sigma}_{11}(t;\widetilde{y})}{\partial t}\Big/\frac{\partial\widetilde{\varepsilon}_{11}(t;\widetilde{y})}{\partial t}\right] \tag{5.5}$$

is next to impossible to be accurately evaluated from the scattered numerical experimental stress and strain data. This is particularly true in the neighborhood of $t \to 0$, which is accompanied by

$$\lim_{t\to 0}[\sigma_{ij}(t;\widetilde{y}),\varepsilon_{ij}(t;\widetilde{y})] \;\to\; 0 \tag{5.6}$$

If the two state variable functions in (5.5) were known precisely - which they are not - then L'Hôpital's rule [74] must be invoked in conjunction with Eqs. (5.3) and (5.4). An identical procedure applies in those instances where the loading functions and their strain/displacement responses are modeled as Heaviside functions, except that in this instance the limit needs to be changed to $t \to 0^+$ in order to avoid the discontinuity at the origin.

Instead one needs to resort to dynamic wave experiments in an isothermal isotropic prismatic rod. The viscoelastic analysis in [5] demonstrates that prior to reflection the 1–D wave front in the x_1-direction moves at an elastic velocity given by

$$\begin{matrix}\text{elastic or viscoelastic}\\ \text{wave front velocity:}\end{matrix}\quad \widetilde{v}_{WF}(\widetilde{y}) \;=\; \sqrt{\frac{\widetilde{E}^0(\widetilde{y})}{\widetilde{\rho}(\widetilde{y})}} \tag{5.7}$$

Consequently, one needs to only measure the wave front velocity $\widetilde{v}_{WF}(\widetilde{y})$ and material density $\widetilde{\rho}(\widetilde{y})$. This is accomplished by performing a hammer impact experiment on a uniform isothermal bar. Depending on the force arrangement, either 1–D tension or compression displacement waves may be generated. The required instrumentation is limited to the hammer force, the two accelerometer outputs and time as shown in Figs. 10 and 11. The wave front velocity is determined from the distance between the two accelerometers and the time difference when the displacement wave fronts first reach each accelerometer. Further details may be found in [50].

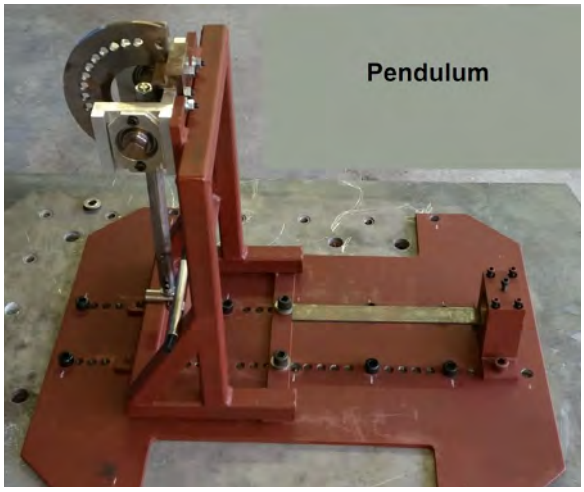

Fig. 10 Typical impact hammer equipment developed at IMI [50]

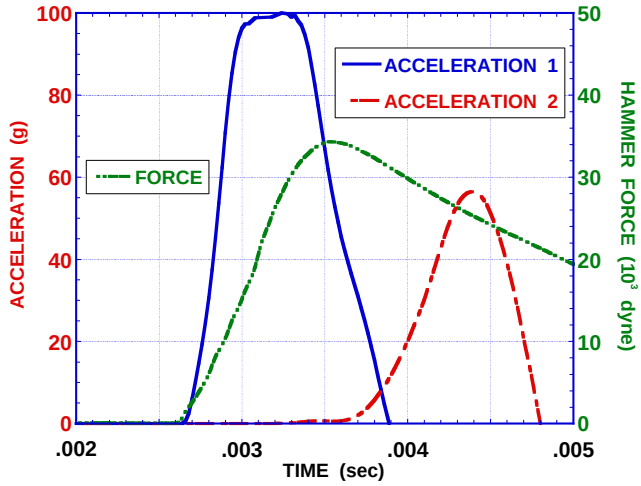

Fig. 11 Readings of accelerations from the two accelerometers and of the compressive impact force [50]

Parenthetically, it may be added that further separate analysis of wave propagations in geometrically identical nonlinear viscoelastic bars [101], demonstrates that the viscoelastic wave front moves at the equivalent linear elastic velocities prescribed by (5.7).

5.4.2 *Torsionally induced shear stresses*

Similar torsional experiments can be conducted on a circular cylindrical specimen by restraining one end and attaching a plate to the other end with a "rigid" moment arm that the hammer impacts to produce a torque. Results from such experiments produce trustworthy values of the instantaneous elastic shear modulus G^0. The simultaneous application of 1–D tension or compression and torsional shear stresses requires high precision load, loading rates and timing application with tight control over the process. This can generally be achieved only through the design and construction of special loading jigs with sensors and actuators.

6 THE MARRIAGE OF ANALYTICAL FORMULATIONS AND EXPERIMENTAL DATA

6.1 The deterministic protocols

6.1.1 *Deterministic Prony series*

From data collections discussed in Section 5, one can readily determine the Prony series parameters E_{ijkln} and τ_{ijkln} defined in (3.37) and (3.38). For each experiment, using Eqs. (5.1) and (5.2) two avenues are open, namely (a) compute both sets of parameters by LSQ fits or (b) on a logarithmic time scale evenly space τ_{ijkln} and determine the E_{ijkln} by LSQ fits. In either case, the appropriate value of the number of parameters N is settled by trial and error based on the desired accuracy in the LSQ fit.

In either procedure the initial instantaneous elastic modulus/compliance cannot be determined with any degree of confidence from quasi-static experiments, such as creep, relaxation, etc. Instead dynamic experiments such as those described in Section 5.2 must be undertaken.

6.1.2 *LSQ protocol for matching any deterministic quasi-static data with Prony series moduli and compliances*

For each individual quasi-static experiment consider the general linear deterministic viscoelastic constitutive relations of Eqs. (3.24) and their 1–D isotropic form (3.31). As a space saving measure only the latter will be discussed. Furthermore for convenience, the loading history of $\sigma_{11}(x,t)$ may be segmented into a number of unequal time intervals t_m with $m \in [1,\ M]$ and $t \in [-\infty,\ \infty]$. The 1–D constitutive relation for such a loading history can then be written as

$$\sigma_{11}(x,t) \ = \ \sum_{m=1}^{M-1} \int_{t_m}^{t_{m+1}} E(x, t_{m+1} - t') \frac{\partial \varepsilon_{11}(x,t')}{\partial t'} \, dt' \quad \text{with} \quad t_m, t \in [-\infty,\ \infty] \tag{6.1}$$

A summary of the steps to establish the Prony series coefficients and relaxation times to match the experimental data are

[i] Substitute the Prony series of (3.36) into (6.1)
[ii] In order to avoid numerical differentiation of experimental data in (6.1), integration by parts should be executed.

[iii] Perform least square analysis (LSQ) on Eqs. (6.1) and experimental data. Either assume τ_n as equidistant on $\log t$ scale and solve for E_n or solve for both E_n and τ_n. Integrals may be directly evaluated numerically by using the numerical experimental data or analytically by generating analytic functions for the $\varepsilon_{11}(x,t)$ experimental data.

[iv] Note that the entire procedure is conducted in the real time domain and there is no need for integral transforms such as LT or FT.

[v] These LSQ procedures are identical when compliances are characterized.

[vi] Additional details on these protocols may be found in [50]

6.1.3 *Deterministic spectral functions*

The spectral function representation of viscoelastic moduli has been analyzed in [63 – 72] and the treatment to follow is a generalization for arbitrarily shaped spectra.

The analytical generation of continuous spectral functions to mimic the graphics of Fig. 5 for $E^{\tau}(\tau)$ or other moduli, compliances, etc., and similar shapes can proceed as follows:

a - For each experimentally determined modulus, generate the Prony series outlined in Section 6.1.1. Such an expression essentially constitutes the spectral function $E^{\tau}(\tau)$ defined peace wise at N discreet τ values

b - Select appropriate spectral functions. For instance, truncated Laurent power series [75] of the type

$$E^{\tau}(\tau) = \begin{cases} \sum\limits_{m=1}^{M_1} E_m^{\tau 1}\,\tau^m & \tau \in [0,\ 1] \\ \\ \sum\limits_{m=1}^{M_2} E_m^{\tau 2}\,\tau^{-m} & \tau \in [1,\ \infty] \end{cases} \qquad \text{with} \qquad 2 < M \leq N-2, \quad \tau \in [0,\ \infty] \tag{6.2}$$

should prove useful for each data set. See (6.3). Although possibly more rapidly convergent truncated series or one with an improved fit may serve better depending on the shape and scatter of the experimental data.

c - Distinct piece wise continuous functions in different regions of $\tau \in [0,\ \infty]$ may also be chosen. By referring to Fig. 5 and to (6.2), one may construct $E^{\tau}(\tau)$ in the positive half infinite τ space as follows

$$E^{\tau}(\tau) = \begin{cases} E_1^{\tau}(\tau) = \sum\limits_{m=1}^{M_1} E_{1m}^{\tau}\,\tau^m & \tau \in [0,\ 1] \\ E_2^{\tau}(\tau) = \sum\limits_{m=1}^{M_2} E_{2m}^{\tau}\,\tau^{-m} & \tau \in [1,\ \tau_{max}] \\ E_3^{\tau}(\tau) = \sum\limits_{m=1}^{M_3} E_{3m}^{\tau}\,\tau^{-m} & \tau \in [\tau_{max},\ \tau_R] \\ E_4^{\tau}(\tau) = 0 & \tau \in [\tau_R,\ \infty] \text{ and } \in [-\infty,\ 0] \end{cases} \tag{6.3}$$

with $E^{\tau}(\tau)$ reaching its maximum value at τ_{max}. The advantage of the above half Laurent series [74], [75] is that they are universally capable of mimicking any piecewise continuous function with high degrees of accuracy. However, other series - such as orthogonal polynomial, Fourier, etc. - may converge more rapidly, but the relative merits of their performances can only be ascertained on a case by case basis.

d - The $E_i^{\tau}(\tau)$ functions must satisfy the following segmented BCs in order to assure smooth transitions between functions in the τ space and to enforce proper starting, transitional and terminating conditions

$$E_1^{\tau}(0) \;=\; \left.\frac{dE_1^{\tau}(\tau)}{d\tau}\right|_{\tau=0} \;=\; E_2^{\tau}(\tau_R) \;=\; \left.\frac{dE_2^{\tau}(\tau)}{d\tau}\right|_{\tau=\tau_R} \tag{6.4}$$

$$E_1^{\tau}(\tau_{max}) \;=\; E_2^{\tau}(\tau_{max}), \qquad \left.\frac{dE_1^{\tau}(\tau)}{d\tau}\right|_{\tau=\tau_{max}} \;=\; \left.\frac{dE_2^{\tau}(\tau)}{d\tau}\right|_{\tau=\tau_{max}} \;=\; 0 \tag{6.5}$$

e - Perform a LSQ operation to determine the coefficients E_{1m}^{τ} and E_{2m}^{τ}, and increase M_i within data availability limits $M_i \leq N_i - 2$ until the best fit is obtained for each power series.

f - Alternately to the LSQ protocol, the coefficients of the truncated Laurent series in (6.2) and (6.3) can be determined by using their formal definitions

$$E_m^{\tau 1} \;=\; \frac{1}{2\pi}\int_0^1 E^{\tau'}(\tau')\,\tau'^{-(m+1)}\,d\tau' \qquad \text{and} \qquad E_m^{\tau 2} \;=\; \frac{1}{2\pi}\int_1^{\infty} E^{\tau'}(\tau')\tau'^{(m-1)}\,d\tau' \tag{6.6}$$

For each experiment, the discrete experimental values of $E^{\tau}(\tau)$ determined from (3.24) to (3.29) are used and the integrations of Eqs. (6.6) are performed numerically. In effect, this parallel procedure based on the same experimental data establishes the equivalence relations between Prony series and spectral modulus/compliance representations.

6.2 The statistical and probabilistic protocols

6.2.1 *Analytical relations and experimental data fits based on statistical moments*

The analytical Weibull, Gauss, log normal, beta, etc., PDFs all possess associated algebraic expressions for statistical moments, i.e. mean, variance, skewness, kurtosis, etc. Since most PDFs involve two parameters only the two moments can be used to match the experimental data. Consequently, the mean $\mu(t)$ and standard deviation $\sigma_{SD}(t)$ of the experimental quasi-static modulus are calculated. Then using the expressions for these moments [74], the various parameters, such as $\alpha(t)$ and $\beta(t)$ for the beta PDF, are established for each PDF. This procedure is undertaken at pre-selected constant times and the appropriate time functions for $\alpha(t)$, etc., are then generated by LSQ fits from these discreet parametric values.

6.2.2 *Analytical relations and experimental data fits based on least square procedures (LSQ)*

A significantly more accurate procedure is to gather all experimental data and obtain the deterministic moduli functions for each specimen. Then at selected constant times perform a LSQ fit in order to calculate the specific PDF parameters at these times. From these discrete sets of parameters establish the time functions for the PDF parameters through another set of LSQ fits of their PDFs.

For example, the beta PDF of Eq. (3.18) for M observed values $X_m(t_\ell)$ with $m = 1, 2, \cdots, M$ at discrete observed times t_ℓ can be rewritten

$$\text{for } \widetilde{X}_m(t_\ell) \in (0,\ 1) \text{ and } \ell = 1, 2, \cdots, L \text{ as} \qquad \log\left[\widetilde{\phi}\left(\widetilde{X}_m; \alpha(t_\ell), \beta(t_\ell)\right)\right] \;=$$
$$-\log\left(B\left[\alpha(t_\ell), \beta(t_\ell)\right]\right) \;+\; \left[\alpha(t_m) - 1\right]\log\left[\widetilde{X}_m(t_\ell)\right] \;+\; \left[\beta(t_\ell) - 1\right]\log\left[1 - \widetilde{X}_m(t_\ell)\right] \tag{6.7}$$

This process generates discrete paired values of the exponents $\alpha(t_\ell)$ and $\beta(t_\ell)$ at times t_ℓ from which the corresponding functions $\alpha(t)$ and $\beta(t)$ can be established by a second LSQ fit. The same process with a different appropriate Eq. (6.7) can be used for any other PDF with any number of parameter time functions. See [50] for more details.

6.2.3 *Matching dynamic and quasi-static statistical E^0s*

Once the experimental quasi-static and dynamic data has been harvested, then one can proceed with the following protocol:

(a) - Select the same preferred PDF for the dynamic and quasi-static data sets.
(b) - Using the dynamic E^0 data produce a LSQ fit for the selected PDF.
(c) - Match each dynamic $\widetilde{E}^0(\widetilde{y})$ with the corresponding quasi-static modulus curve $\widetilde{E}(0;\widetilde{y})$ at corresponding $\widetilde{y}$s and replace the initial moduli.
(d) - Recompute the quasi-static data Prony series coefficients based on the dynamic $E^0(\widetilde{y})$ values. These are now the proper modulus Prony series based on available experimented data.

6.2.4 *Random spectral moduli and compliances*

Moduli and compliances that are represented by spectral functions are best categorized by Formulation A of Section 3.5.1. The complexities of Formulations B and C render the latter excessively cumbersome and hence impractical. The procedure for determining the appropriate PDF and matching its parameters to the statistical data is identical to that prescribed above for the Prony series characterization since in both configurations the PDF is an entirely separate function from the deterministic modulus and compliance rendering.

7 EXPERIMENTAL METHOD FOR SHORT TERM CREEP AND TENSION TESTS AT DIVERSE TEMPERATURES

7.1 General failure considerations

Viscoelastic material failures are inherently time-dependent and there are a number of state variables that contribute to failure times, namely ultimate stresses, ultimate strains, temperatures and moisture. Consequently, diverse opportunities offer themselves for conducting creep experiments at different temperatures under one of the following conditions:

1 - X% of ultimate stresses
2 - Y% of ultimate strains
3 - Z% of ultimate (survival) times
4 - Same stress at failure
5 - Same strain at failure
6 - Same time at failure
7 - Same dissipative energy level at failure

Even though the material is linear, except when approaching the failure region, they all have different creep rates and histories because they involve different terminal points on the modulus-time curves. Viscoelastic material fatigue generally is not a problem because the exceedingly high numbers of failure cycles take longer to reach than the survival creep/relaxation times listed above.

Tension coupons made of thermoset vinyl ester resin (VER), DERAKANE® 441-400 by Ashland Co., with a styrene content of 33% by weight were subjected to short term tensile creep tests per ASTM D 638-99 [109]. Ten specimens were tested at three temperatures (24°C, 40°C and 60°C) at 70% of their ultimate tensile loads $\sigma_u(t,T)$. The test temperature levels were below the polymer's glass transition temperature of 135°C. Isochronous curves were developed for all temperatures to establish linearity so that a linear viscoelastic analysis could be used. The test temperature-stress pairs for the short-term tension experiments are shown in Fig. 12. The strain time histories were obtained through digital image correlation as the test articles were subjected to a steady applied stress for two hours, followed by one hour recovery.

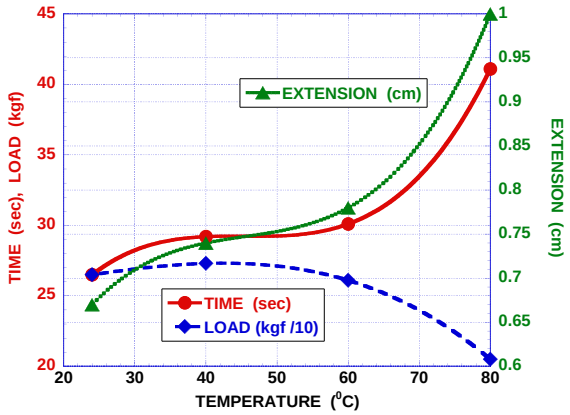

Fig. 12 Ultimate stresses, strains and temperatures for DERAKANE®. Tension tests are marked [60].

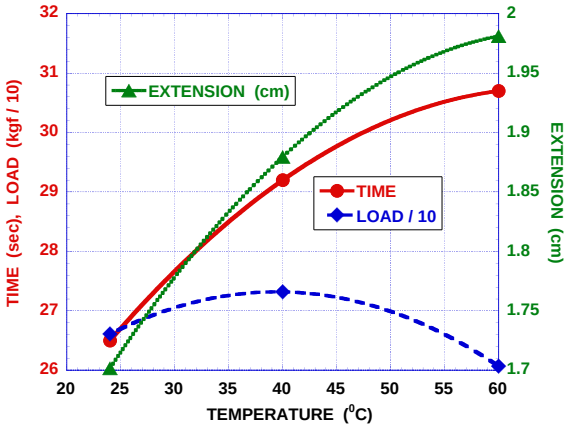

Fig. 13 Ultimate conditions in tension for DERAKANE® at constant elongation rate [60]

The results depicted in Figs. 12 and 13, while for the same material, are under different imposed loading conditions and hence not directly comparable with each other. An examination of these plots indicates decreasing ultimate tension stresses in creep and increasing times to reach them in tension as a function of increasing temperatures. The first condition is not unexpected while the second may appear as a contradiction until one takes note of the fact that these tension tests were all conducted under identical elongation time rates while taking longer to reach the larger ultimate strains.[15]

However the tension experiment situation is more complicated as there are a number of other contributors. Consider the implications of the constitutive relations (3.24) and (3.25). For TSM of Section 4.1 the modulus and compliance time derivatives are insensitive to temperature changes, but $E(t)$ and $C(t)$ curves shift in a parallel fashion on the time axis. For this material the observed failure strains increase with ultimate time and the combinations of longer failure times to rupture produce larger ultimate strains. The latter would indicate that sufficient creep strains are developing to maintain constant extension rates but that creep is insufficiently large to increase elongations at similar time rates.

The change in failure extension values with time and temperature is plausible as the latter at a time t are given by the integral relation

[15] Elongation/extension rates were maintained as constants except for loading and unloading periods - see Fig. 8 and Eqs. (5.3).

$$\Delta L(t) \;=\; \int_0^t \int_0^{L_0+\Delta L(t)} \varepsilon_{11}(x_1,t')\,dx_1\,dt' \approx \int_0^t \int_0^{L_0} \varepsilon_{11}(x_1,t')\,dx_1\,dt' \tag{7.1}$$

where $\Delta L(t)$ is the change in total specimen length. Generally, strains are measured only at the x_1 position where necking occurs and the longitudinal distribution of $\varepsilon_{11}(x_1,t)$ is unavailable for the remaining entire specimen length. Hence, the integration of (7.1) cannot be carried out based on available experimental data.

It should also be noted that the tension failures are nonlinear phenomena as they involve necking with the accompanying reduction in cross sectional area even if the constitutive relations should remain linear. The latter only affects stress calculations. The area time function is governed by the specific linear or nonlinear constitutive relations. All other state variables - load $F(t)$, elongation and time. - were obtained from direct experimental measurements.

For an isotropic material and 1–D loading, strains in the two directions normal to the loading one are equal, i.e. $\underbrace{\varepsilon_{22}(x_1,t) = \varepsilon_{33}(x_1,t)}_{\text{not measured}} \neq \underbrace{\varepsilon_{11}(x_1,t)}_{\text{measured}}$. The cross sectional area $A(x_1,t)$ then is

$$A(x_1,t) \;=\; A_0 + \Delta A(x_1,t) \;=\; [1+\varepsilon_{22}(x_1,t)]\,[1+\varepsilon_{33}(x_1,t)]\,A_0 \;=\; [1+\varepsilon_{22}(x_1,t)]^2\,A_0 \tag{7.2}$$

The tension experiments were conducted prior to the delivery of the digital image correlation (DIC) equipment and should be considered exploratory in nature. Thus, only loads, mechanical extensometer extensions and strains in the loaded direction could be measured over the 1 in gage length. Consequently, calculations for $\Delta A(t)$ and the "true" stresses at the rupture point

$$\sigma_{11}(x_1,t)\Big|_{x_1=L(t)/2} \;=\; \frac{F(t)}{A_0(x_1 t) + \Delta A(x_1,t)}\bigg|_{x_1=L(t)/2} \quad \text{with} \quad \frac{dA(x_1,t)}{dt}\bigg|_{x_1=L(t)/2} < 0 \tag{7.3}$$

cannot be carried out. Hence, Figs. 12 and 13 present, among other state variables, the measured applied tension force $F(t)$, extension, time and temperature.

On the other hand, linear theory, of course, implies that

$$\varepsilon_{\underline{ii}}(x,t) \;\ll\; 1 \qquad \Delta A(x,t) \;\ll\; A_0(x,t) \qquad L(t) \;\approx\; L_0 \tag{7.4}$$

thus greatly simplifying the analysis except in the neighborhood of the stress rupture where it is incapable of accurately predicting failure due to necking. Separately, it does not apply to any large strains of $\varepsilon_{ij} \gtrapprox 0.1$ prior to any failures.

7.2 Measured creep strains and corresponding spectral function

Consider next another distinct class of material property determining experiments. The longitudinal creep strain histories are shown in Figs. 14 for all test temperatures. As expected, the creep deformation in the loading direction increases monotonically with increasing time, stress level, and temperature, particularly during the steady state creep phase ($t \geq 1000$ s). These figures also demonstrate the variability of the measured strain, for the same material, environmental conditions and test methodology.

A spectral function approach was used to express the viscoelastic responses. This development is covered in more detail in [68], [70] and Sections 3.3 and 6.1.3. A brief overview with a specific illustrative example function is given in this section for completeness.

For a linear viscoelastic material, the strain and stress time histories can be obtained from (3.24) and (3.25). Anisotropic spectral compliances then become

$$C_{ijkl}(x,t) \; - \; C^{\infty}_{ijkl}(x) \; = \; - \; \lim_{N\to\infty} \left\{ \sum_{n=1}^{N} C_{\underline{ijkl}n}(x) \exp\left(\frac{-t}{\tau_{\underline{ijkl}n}(x)} \right) \right\} \; \to$$

$$- \int_0^{\infty} \underbrace{C^{\tau}_{ijkl}(x,\tau) \exp\left(\frac{-t}{\tau} \right)}_{= C^{s\tau}_{ijkl}(\tau;x,t)} d\tau \; = \; - \int_0^{\infty} \underbrace{\frac{C^{*\tau}_{ijkl}(x,\tau^*)}{\tau^*} \exp\left(-t\,\tau^*\right)}_{= C^{*s\tau}_{ijkl}(\tau^*;x,t)} d\tau^* \; = \; - \, C^{sp}_{ijkl}(x,t) \tag{7.5}$$

for $\tau = 1/\tau^*$ and with the spectral instantaneous compliances given by

$$C^{0}_{ijkl}(x) \; = \; C^{\infty}_{ijkl}(x) \; - \; \int_0^{\infty} C^{\tau}_{ijkl}(x,\tau)\, d\tau \tag{7.6}$$

Isotropic materials are defined by only two compliances $C_{1111}(x,t)$ and $C_{1122}(x,t)$. Separately, but not independently, a 1–D compliance $C(x,t)$ is also available. The corresponding relaxation moduli are similarly defined. For the current study, the vinyl ester (VE) polymer is taken to be an isotropic material and the spectral $C^{\tau}_{ijkl}(x,\tau)$ functions are selected as [70]

$$C^{\tau}_{ijkl}(x,\tau) \; = \; \frac{C^{\tau}_{ijkl}(x)}{\pi\left(1+n_0^2\tau^2\right)} \tag{7.7}$$

Using the spectral function from (7.7) for an isotropic material subjected to a 1–D loading, $\sigma_{11}(x,t) \neq 0$, and applying the elastic-viscoelastic correspondence principle and Laplace transforms, yields strains as given by the Volterra integral equation [70]

$$\varepsilon_{\underline{ii}}(x,t) \; = \; \underbrace{C^{0}_{11\underline{ii}}(x)}_{\substack{\text{instantaneous} \\ \text{compliances}}} \sigma_{11}(x,t) \; + \; \frac{C^{\tau}_{11\underline{ii}}}{\pi} \int_0^{t} \left(\sigma_{11}(x,t-t') \int_{n_0 t'}^{\infty} \frac{\cos(z-n_0 t')}{z}\, dz \right) dt' \tag{7.8}$$

Similarly, using (7.7) a spectral expression can be derived for the relaxation moduli that yields

$$E_{11\underline{ii}}(x,t) \; = \; E^{0}_{11\underline{ii}}(x) \left[\left(1 - \frac{m_{\underline{i}}}{2}\right) + \frac{m_{\underline{i}}}{\pi} \int_{n_{0_{\underline{i}}} t}^{\infty} \frac{\sin(z-n_{0_{\underline{i}}} t)}{z}\, dz \right] \qquad m_i \; = \; \frac{n_{\underline{i}}}{n_{0_{\underline{i}}}} \tag{7.9}$$

The moduli derived from each test and at constant temperature levels is depicted in Fig. 15.

7.3 Statistical analysis of relaxation moduli

Two parameter Weibull, log normal and beta PDFs were used to develop the probability distributions of the relaxation moduli for all tests at each time. These PDFs $\widetilde{\phi}\left[\widetilde{y}, \boldsymbol{k}(t)\right]$ are listed in Section 3.1.2. Ten relaxation moduli at each time were used to determine the Weibull, log-normal and the beta

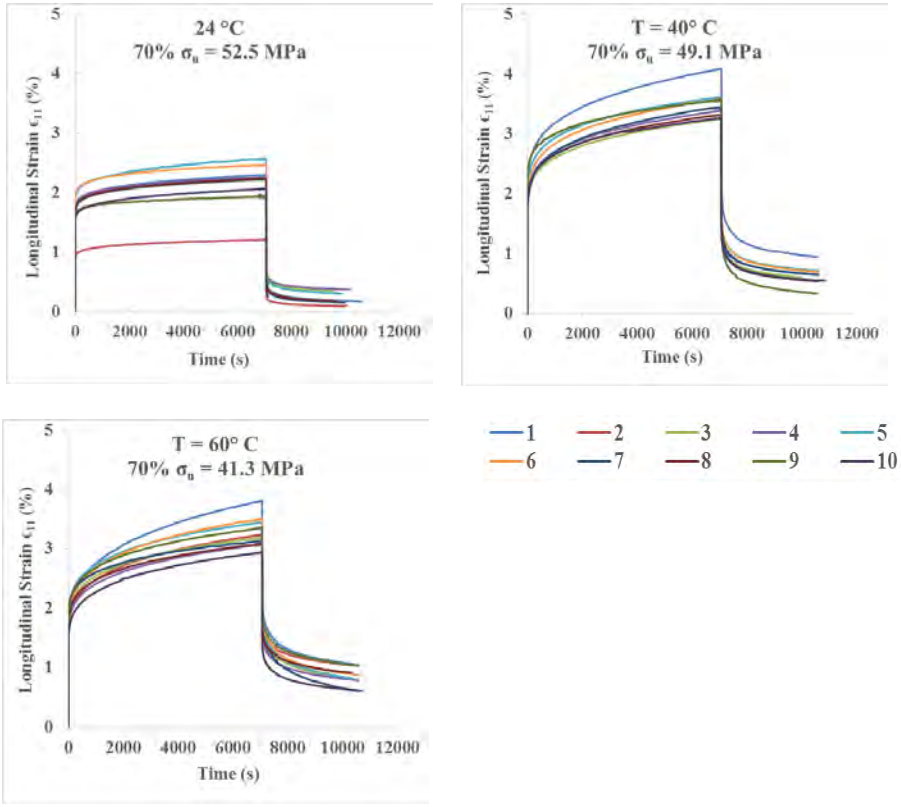

Fig. 14 Longitudinal creep/creep recovery responses of ten cured DERAKANE® 441-400 specimens at 70% σ_u at T = (a) 24°C, (b) 40°C and (c) 60°C

parameters. The observation data vector $\widetilde{y}$ represents the ten relaxation modulus values $(N_0 = 10)$ at each time in the interval $0 \leq t \leq 7000$ s.

The LSQ protocol for matching functional parameters to experimental data is described in Section 6.2. Alternately, PDF parameters may be determined by matching statistical moments obtained from data with those dictated by the analytical PDFs. It must be emphasized that when the pertinent parameters are determined for each selected PDF, they lose their physical identity and simply become players to produce best LSQ fits of the experimental data. Consequently, they generally do not reflect true physical values of, for instance, standard deviations, etc. The ultimate comparisons of the selected PDFs, therefore, does not rest with these parameters nor with the corresponding PDFs but with the CDFs since they are proper representative of the final product to be used in material response predictions.

7.4 Time and temperature dependency of the PDF parameters

The relaxation modulus statistical results from these analyses described in Section 7.3 are displayed in Figs. 16 and 17. The DERAKANE® 441-400 VER experiments were conducted at 70% of ultimate stresses, the latter being temperature-dependent.[16] This results in $\sigma_u - T$ couplings of 52.5MPa – 24°C, 49.1MPa – 40°C and 41.3MPa – 60°C. The match between experimental values and analytical

[16] See Figs. 12 and 13.

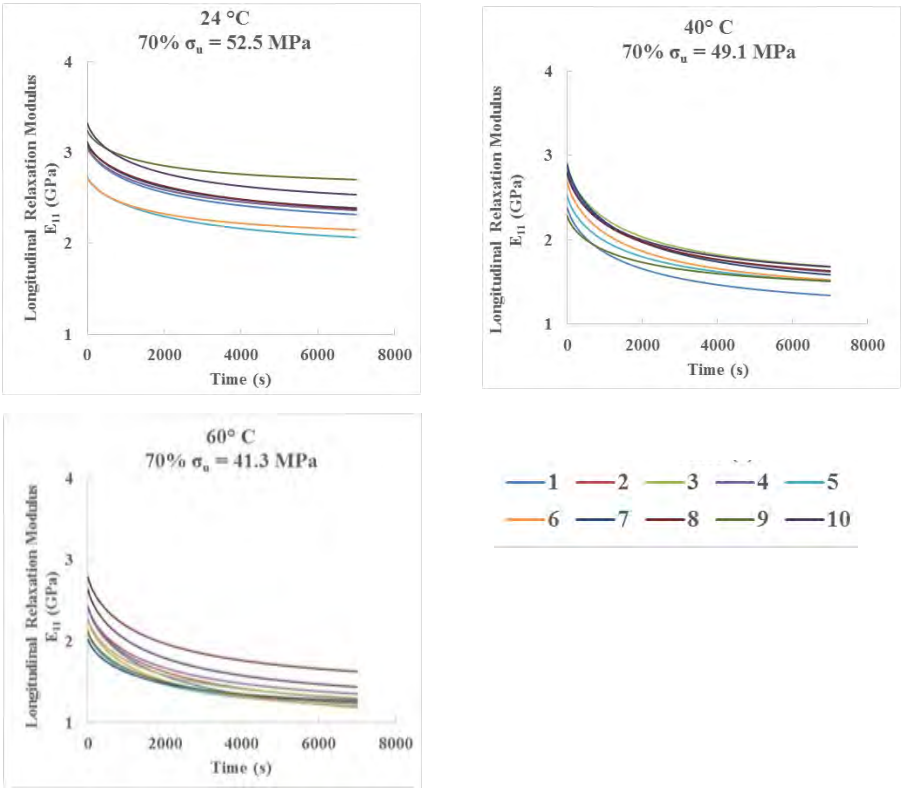

Fig. 15 Relaxation modulus of ten cured DERAKANE® 441-400 specimens at 70% σ_u at T = (a) 24℃, (b) 40℃ and (c) 60℃

PDFs was accomplished by using means and variances at each time and temperature obtained from the experimental data. The computations were based on maximum likelihood estimations [110].

Figs. 16 – 18 represent the PDFs and CDFs associated with the statistical relaxation modulus data of the previous two figures. They are limited to a specific time, namely occurrences at $t = 3000$s and similar graphics can be produced at each desired time. The first two statistical moments are displayed in Table 1.

Statistics ⇓ / Temperature ⇒	24℃	40℃	60℃
mean (μ) ⇒	0.556	0.708	0.317
standard deviation (σ_{SD}) ⇒	0.270	0.257	0.338

Table 1 Relaxation modulus statistics from ten experiments at 3000 s

By and large, the PDFs and CDFs in Figs. 16 to 18 look "reasonable" except for the beta PDF in Fig. 16(d). The apparent departure to unbounded regimes is capped by the PDF's limits at $y = 0$ and 1 as seen in Section 9. They are due to the parameter values of $\alpha(t)$ and/or $\beta(t) \in (0,\ 1)$. Although

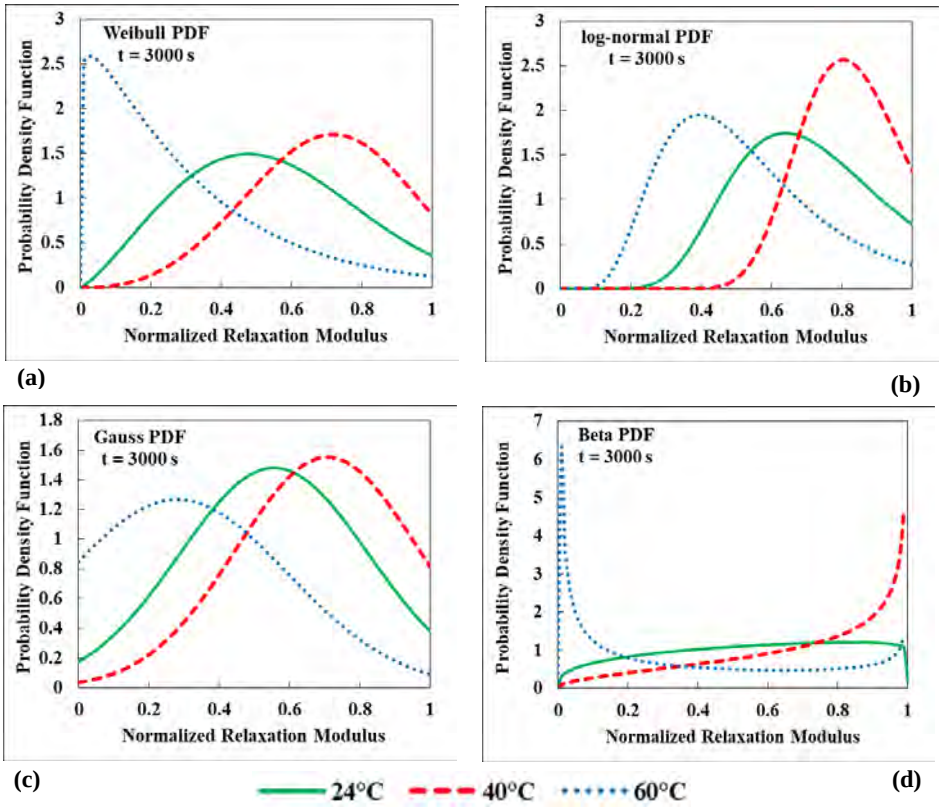

Fig. 16 (a) Weibull, (b) log-normal, (c) Gauss and (d) beta probability density functions (PDF) at $t = 3000$ sec

some of the PDFs in Fig. 16 look different from each other, the CDFs in Figs. 17 and 18, except for the log-normal CDF, resemble each other much more closely.

Also see Figs. 1 to 3 for a different polymer's probabilistic results. In both examples, i.e. for both materials, the number of samples is too small to provide sufficient statistics – see Eqs. (3.2) to (3.7) – and results are exhibited only to illustrate the necessary protocols that weld the experimental data to the analytical representations.

8 DISCUSSION AND CONCLUSIONS

8.1 General observations

Fig. 19 is a composite schematic or flow chart of the deterministic and statistical analytical and experimental protocols needed for the determination of viscoelastic moduli and compliances. Its intent is to summarize the formulation and development route to viscoelastic constitutive relation characterization.

The analytical and experimental formulations contained herein are solely devoted to constitutive relations and failure characterizations are not included. Current failure theories – or lack thereof – indicate that they are independent of constitutive relations per say, except for stress and strain levels encountered in actual situations.

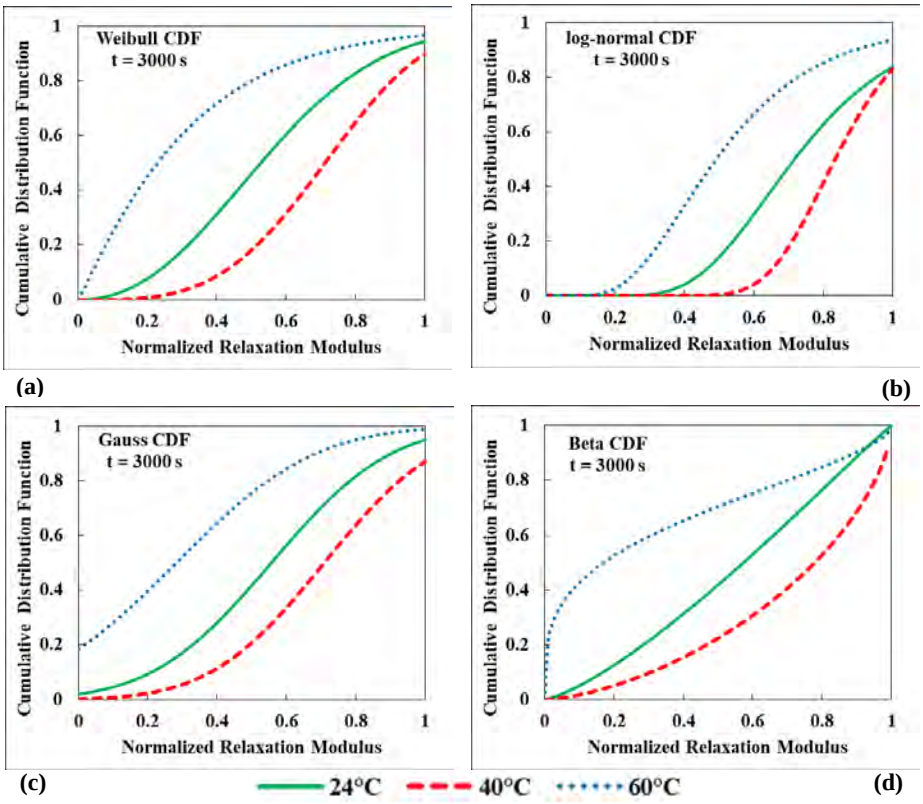

Fig. 17 (a) Weibull, (b) log-normal, (c) Gauss and (d) beta cumulative distribution functions (CDF) at $t = 3000$ sec

There are at least two major caveats to consider in connection to the dynamic wave experiments, namely (a) - the times between wave front arrivals at the two accelerometers is extremely short, $O(10^{-3})$ secs, and (b) the distance between accelerometers is small, $\approx$ 20 cm, for a bar length of 30.4 cm. The need for a short bar is to prevent bending under its own weight in order to preserve the integrity of the 1–D formulation. Sensitivity studies in [50] have shown that a $\pm 10\%$ variation in velocity and in density measurements can produce a 61% variation in E^0.

The demonstrated sensitivity of viscoelastic media to starting transients and the physically unachievable Heaviside function loadings dictate that adequate functionality of starting stresses, strains and displacements as well as of material properties should be included in quasi-static and dynamic phenomena.

Loading conditions other than creep and relaxation such as constant strain rates after the initial loading cycles have been shown to be less than useful because of early material failures due to excessive total strains [50], [102 – 108]. Such relatively short time experiments fail to cover the time span to the point where the material has been fully relaxed and thus are inadequate to produce valid Prony series coefficients. The utility of any PDF is governed by its ability to accurately represent statistical data and its satisfaction of the proper sufficiency conditions, such as (3.2) and (3.5) for example.

Three possible random PDF models for material property characterization are presented. Formulation A is the simplest and should be considered as the candidate of practical choice. The sophistications introduced by the other two formulations are unnecessary because viscoelastic material data is highly scattered and the number of experimental samples are generally too few for adequate statistics.

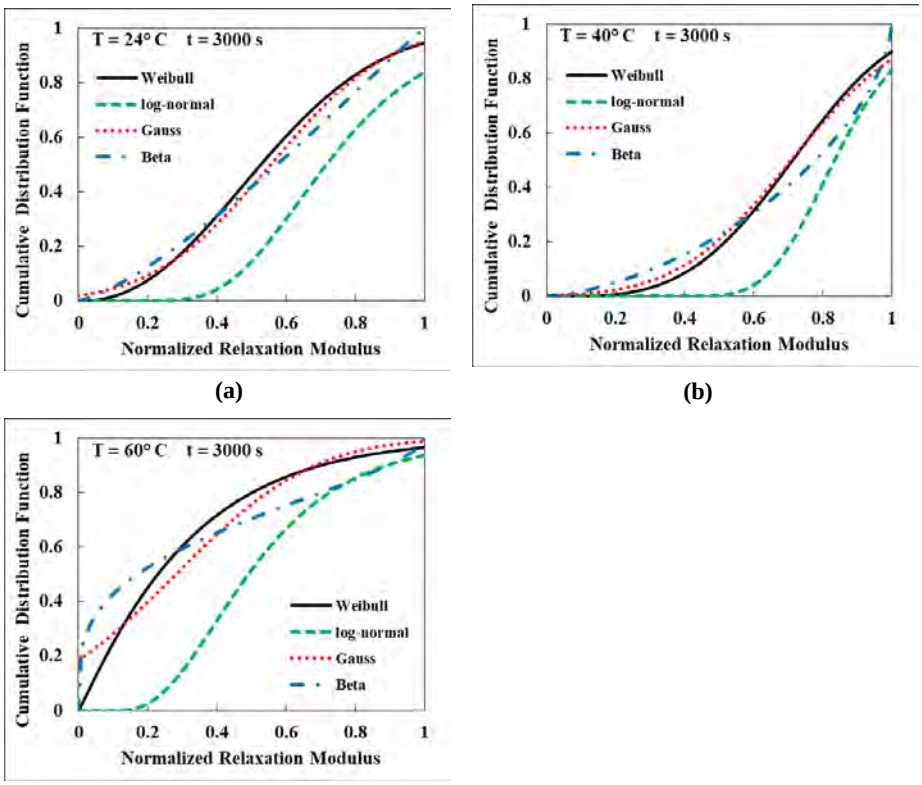

Fig. 18 Composite (a) Weibull, (b) log-normal, (c) Gauss and (d) beta cumulative distribution functions (CDF) at $t = 3000$ sec

Currently, due to the inability to manufacture high polymers and other viscoelastic materials with any semblance of material property repeatability points to prevailing conditions where the application of highly complicated statistics is unwarranted.

Once the PDF is selected and its parameters are established in agreement with the experimental statistical data, then the expected value $\boldsymbol{E}$ for moduli, compliances, temperatures, shift functions, stresses, strains, etc., at any point x at time t can be established by

$$\boldsymbol{E}\left[\widetilde{E}_{ijkl}\left(\widetilde{y};x,t\right)\right] = \int_{-\infty}^{\infty} Y\,\widetilde{E}_{ijkl}(Y;x,t)\,dY \tag{8.1}$$

provided the integral exists.

The introduction of deterministic or stochastic temperatures and/or TSM time-temperature shift functions greatly complicates material characterization and subsequent stress analyses, however the inclusion is unavoidable because of the severe dependence of viscoelastic material properties on temperatures. Viscoelastic numerical solutions employ finite element methods (FEM) or recurrence relations. For large FEM and numerical time integration problems, the comparative computational advantages and disadvantages of Prony series vs. spectral function characterizations must be evaluated on a case by case basis. The combinations of spatial FEM and time integrals may be carried out by methods presented in [111] – [117].

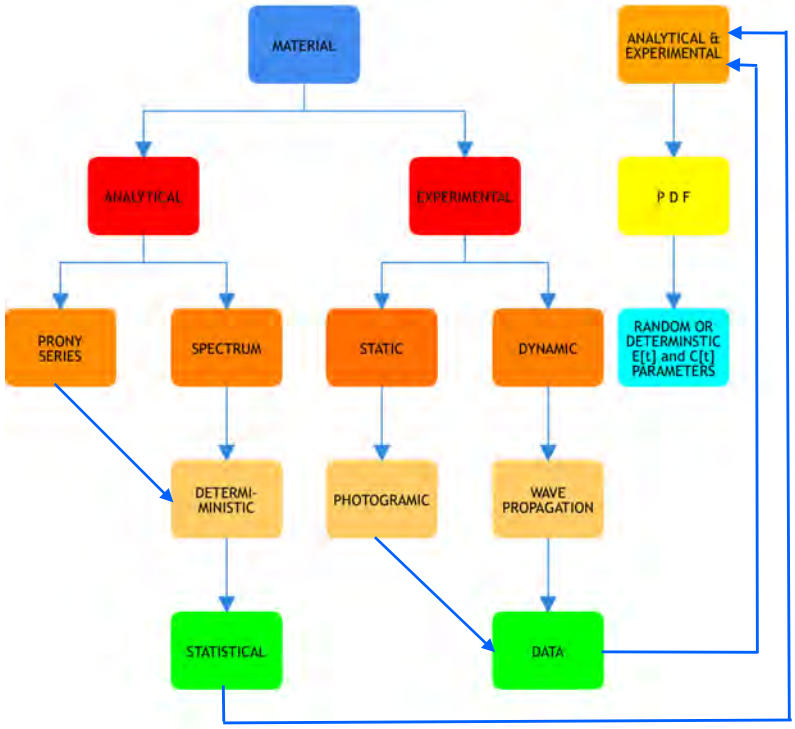

Fig. 19 Flow chart for analytical and experimental material property determinations

The relaxation modulus spectral treatments formulated here are generalizations in terms of arbitrary functions built on previous developments as reported in [63 – 72]. One of the notable features of spectral representations is their direct relation to Laplace and Fourier transforms thus facilitating their analytic characterizations. However, the Prony series exponential functions have relatively simple LTs and FTs as well. In both representations extensive difficulties are encountered at the inversion steps when partial fractions, Post's formula (3.43), inverse fast Fourier transforms (IFFT) [118], etc., need to be employed. Alternately, the transform and their inversion routes can be avoided by carrying out the analysis in real time space, which then involves time integrations at every finite element node.

When modeling the spectral functions, one need not necessarily limit oneself to power series. Other series such as orthogonal polynomials, Fourier, etc., are equally suitable representations of actual spectral properties. From a stress/strain analysis viewpoint the optimum function selection should be a short rapidly converging truncated series that is the least computationally intensive.

8.2 Comparison of three modulus/compliance representations and usages

Various advantages and disadvantages of three characterization approaches are summarized in Table 2. Prony series are straightforward additive combinations of two parameters per term and are the easiest to characterize from experimental data. However, they may require a relatively large number of terms.

The spectral functions are piecewise continuous per Eqs. (5.3) and (6.3) and in principle should be the most faithful characterization. Both Prony series and special renderings of constitutive relations require no time derivatives after integration by parts. This assures best accuracy in matching numerical

Characterization $\Rightarrow$	Prony series	Spectral function	Fractional derivatives
Advantages $\Rightarrow$	exponential series, no derivatives needed	piece-wise continuous functions for $\tau \in [0,\infty]$ no derivatives needed	3 parameter KMs with extra α_n plus E_n^{FD} and τ_n^{FD}
Disadvantages $\Rightarrow$	may need 30 terms 2 parameter KMs (E_n and τ_n)	one extra integration	high order derivatives and N_{ijkl} extra integrations

Table 2 Comparisons of modulus/compliance representations

data to analytic relations because of the notoriously inaccurate numerical data derivatives. However, each spectral constitutive relation requires an additional integration.

Fractional derivatives offer an extra parameter per term to be recovered by LSQ matching of experimental data and their series should, in principle, converge with a smaller number of series terms. However, they also require higher order (up to N_{ijkl}) time derivatives and repeated time integration for each term of the FD series. The former make LSQ matching potentially inaccurate because of the high order numerical time derivatives and cause FEM stress analysis to be CPU intensive due to the required multiples of N_{ijkl} repeated time integrations.

Compared to the Riemann-Liouville definition, the Caputo FD representation is simpler to manipulate by drawing the derivatives directly into the integrand as opposed to differentiating the integrals in toto. The general FD formulations [85] can be significantly reduced in complexity by limiting them only to first order ones ($N_{ijkl} = 1$), but including a set of distinct α_{ijkln}, E_{ijkln}^{FD} and τ_{ikln}^{FD} coefficients for each n term. However, under these conditions each and every α_n parameter is then severely restricted to values $0 < \alpha_n < 1$, see (3.49). These configurations essentially represent Kelvin models (KMs) with Newtonian fluid dashpots with time-dependent viscosity coefficients, but with a distinct third parameter in each series term.

In the final analysis, each modulus representation's contributing advantages and disadvantages must be examined and evaluated on an individual basis tailored to each specific problem and viscoelastic material.

Furthermore, it is important to note that what determines the adequacy of a good functional fit to data is the totality of the CDFs for E_{ijkl}, C_{ijkl}, etc., and not their individual parameters nor their PDFs. The classical example is the matching of a Prony series to experimental data where some of the coefficients turn out negative – a physical prima facia contradiction – but the entire sum adds to a good modulus match. Additionally, since these parameters are determined though LSQ protocols their values reflect best fit conditions and can no longer be associated with their physical identities, such as standard deviations, etc.

8.3 Comments on Weibull, log-normal, Gauss and beta PDF behaviors and idiosyncrasies

Potential problem areas and remedies:

The log-normal PDF at $\widetilde{y} = 0$ requires special computational procedures to avoid phantom numerical singularities where none are present in either the mathematical model (3.12) or physical real world events. Proper programming code must be introduced to assure that

$$\lim_{\widetilde{y}\to 0}\left\{\widetilde{\phi}_{LN}(\widetilde{y},t)\right\} \;=\; \lim_{\widetilde{y}\to 0}\left\{\frac{1}{\widetilde{y}\,\sigma_{LN}(t)\sqrt{2\pi}}\exp\left(-\left[\frac{\ln(\widetilde{y})-\mu_{LN}(t)}{\sqrt{2}\,\sigma_{LN}(t)}\right]^2\right)\right\} \;\to\; 0 \tag{8.2}$$

as well as in its neighborhood when $\widetilde{y} \in (0,\ll 1)$. Here the code logic must lead to results for $\widetilde{\phi}_{LN}$ that are $\ll 1$ and start to continuously build up the PDF_{LN} values as $\widetilde{y}$ increases until they reach a maximum. Then the PDF_{LN} decreases to zero as $\widetilde{y} \to \infty$.

The Gauss PDF suffers from the unrealistic span extension over the entire interval $-\infty \leq \widetilde{y} \leq \infty$. This characteristic is particularly troublesome when the data is significantly scattered with its associated relatively large standard deviations.

The Weibull PDF is unbounded at the origin when $k(t) \in [0,\ 1)$, namely

$$\lim_{\widetilde{y}\to 0}\left\{\widetilde{\phi}_W(\widetilde{y},t)\right\} = \lim_{\widetilde{y}\to 0}\left\{\left(\frac{\widetilde{y}}{\lambda(t)}\right)^{k(t)-1}\exp\left(-\left[\frac{\widetilde{y}}{\lambda(t)}\right]^{k(t)}\right)\right\} \to \infty \quad \text{for } k(t) \in (0,\ 1) \tag{8.3}$$

but its CDF is finite $\forall\ \widetilde{y} \in [0,1]$. Unfortunately, this singularity is not removable by switching to a 3 parameter Weibull PDF as seen in the Appendix of Section 9.

The beta PDF_B has built-in singularities at $\widetilde{y} = 0$ and/or 1 if α or β or both < 1. These less than unit parameter values obtained from data matching stem from two possibilities, namely (a) the matching of mean and variance values causes insufficiently accurate PDF representations and/or (b) there is an insufficient number of data points required to obtain proper mean and variance values - Eqs. (3.2) – (3.7). While there are three roots satisfying Eqs. (3.22), two pairs yield $\alpha(t) = \beta(t) = 0$, which does not satisfy the condition (3.20), namely that each must be positive and real. The first cause can be eliminated by matching the beta PDF_B through LSQ fits and and the second problem can only be alleviated by conducting a sufficient number of additional experiments.

One of the advantages of the LSQ fits is that during any PDF parameter determinations this protocol automatically forces inclusion of the data points at $\widetilde{y} = 0$ and 1.

However, it must be emphasized that even though the Weibull and/or beta PDFs may be unbounded at $\widetilde{y} = 0$ and 1, *the corresponding CDF expressions yield the proper values of* 0 *and* 1 *respectively for* $\alpha(t), \beta(t) \in (0,\ 1)$. *Similarly, the Weibull* PDF_W *has no finite limit at* $\widetilde{y} = 0$ *but its CDF has the proper zero value at the origin.*

Finally when all is said and done, proper probability distributions (CDFs) for the entire interval $\widetilde{y} \in [0,\ 1]$ *are the most important parts of the statistical and probability analyses regardless of any unconstrained PDF behavior patterns.*

A parallel conclusion is equally evident regarding the assembly of modulus/compliance Prony series where the individual parts are unimportant but their sum is of paramount interest.

Based on a limited number of experiments, it would appear that of the four PDFs considered – Weibull, Gauss, beta and log-normal – the last of the quadruple selection is the least accurate in predicting proper CDFs, while the beta one approaches reality by a significant margin.

9 APPENDIX – The 3 parameter Weibull model

This PDF offers one additional parameter available for curve fitting [119]. However, the unbounded physically non-representative situation at the $\widetilde{y}$ origin for $k_1(t) < 1$ is not alleviated if one switches to a 3 parameter Weibull PDF, where essentially the third parameter $k_2(t)$ shifts the PDF curve to the left or right along the $\widetilde{y}$ axis

$$\left.\begin{array}{c}\text{3 parameter}\\ \text{Weibull PDF} \Longrightarrow\\ \widetilde{\phi}_W\left[\widetilde{y};\lambda(t),k_1(t),k_2(t)\right]\end{array}\right\} = \begin{cases} \dfrac{k_1(t)}{\lambda(t)}\left(\dfrac{\widetilde{y}-k_2(t)}{\lambda(t)}\right)^{k_1(t)-1}\exp\left[-\left(\dfrac{\widetilde{y}-k_2(t)}{\lambda(t)}\right)^{k_1(t)}\right] & \widetilde{y}\in\mathbb{R}_{\mathbb{SI}} \\ 0 & \widetilde{y}\notin\mathbb{R}_{\mathbb{SI}} \end{cases} \tag{9.1}$$

$$\left.\begin{array}{c}\text{3 parameter Weibull CDF} \Longrightarrow\\ Pr_{3W}\left[\widetilde{y};\lambda(t),k_1(t),k_2(t)\right]\\ \displaystyle\int_0^{\widetilde{y}}\widetilde{\phi}_{3W}[Y;\lambda(t),k_1(t),k_2(t)]\,dY\end{array}\right\} = \begin{cases} 1-\exp\left[-\left(\dfrac{\widetilde{y}-k_2(t)}{\lambda(t)}\right)^{k_1(t)}\right] & \widetilde{y}\in\mathbb{R}_{\mathbb{SI}} \\ 0 & \widetilde{y}\notin\mathbb{R}_{\mathbb{SI}} \end{cases} \tag{9.2}$$

with $\lambda(t),k_1(t)>0$ and $k_2(t)<0\leq\widetilde{y}\leq 1$. The k_1s and λs respectively remain the shape and scale parameters, while k_2 is the location parameter. These three parameters, like all the others, can be determined either from the first three statistical moments or through LSQ fits.

10 ACKNOWLEDGEMENTS

RWS expresses her thanks to the Aerospace Engineering Department and to the Bagley College of Engineering at Mississippi State University (MSU) in Starkville, MS for support of this research. JS thanks the Aerospace Engineering Department at MSU as well as the Mechanical Engineering Department at Auburn University (AU) in Auburn, AL, for their support. Support for HHH by the Aerospace Engineering Department in the College of Engineering and by the Computing and Data Sciences Division (CDS) of the National Center for Supercomputing Applications (NCSA) at the University of Illinois at Urbana-Champaign (UIUC) is gratefully acknowledged.

REFERENCES

[1] Turner Alfrey, Jr., (1948) *Mechanical Behavior of High Polymers.* Interscience Publishers, Inc., New York.

[2] John J. Aklonis, and William J. MacKnight (1983) *Introduction to Polymer Viscoelasticity*. Wiley, New York.

[3] Georgii M. Bartenev, and Yurri S. Zuyev (1968) *Strength and Failure of Viscoelastic Materials*. Pergamon Press, Oxford.

[4] Bažant, Zdeněk P. (Ed.) (1988) *Mathematical Modeling of Creep and Shrinkage of Concrete*. John Wiley and Sons, New York.

[5] David R. Bland, (1960) *The Theory of Linear Viscoelasticity.* Pergamon Press, New York.

[6] Richard M. Christensen, (1982) *Theory of Viscoelasticity - An Introduction, 2nd ed.* Academic Press, New York.

[7] Aleksey D. Drozdov, (1998) *Mechanics of Viscoelastic Solids.* John Wiley & Sons, New York.

[8] Aleksey D. Drozdov, (1998) *Viscoelastic Structures Mechanics of Growth and Aging.* Academic Press, San Diego.

[9] Mauro Fabrizio, and Angelo Morro (1992) *Mathematical Problems in Linear Viscoelasticity*. SIAM, Philadelphia, PA.

[10] William N. Findley, James S. Lai and Kasif Onaran (1976) *Creep and Relaxation of Nonlinear Materials*. North-Holland Publ. Co., Amsterdam.

[11] Alfred M. Freudenthal, (1950) *The Inelastic Behavior of Engineering Materials and Structures*. John Wiley & Sons, New York.

[12] John M. Golden, and George A. C. Graham (1988) *Boundary Value Problems in Linear Viscoelasticity*. Springer Verlag, Berlin.

[13] Bernhard Gross,(1953) *Mathematical Structure of the Theories of Viscoelasticity.* Hermann & Cie., Paris.

[14] Harry H. Hilton, (1964) "An introduction to viscoelastic analysis," *Engineering Design for Plastics* (E. Baer, ed.) 199–276. Reinhold Publishing Corp., New York.

[15] H. H. G. Jellinek, and R. Brill (1956) "Viscoelastic properties of ice," *Journal of Applied Physics* **27**:1198–1209.

[16] Roderic S. Lakes, (1998) *Viscoelastic Solids.* CRC Press, Boca Rotan.

[17] Roderic S. Lakes, (2009) *Viscoelastic Materials.* Cambridge University Press, New York.

[18] Benjamin J. Lazan, (1968) *Damping of Materials and Members in Structural Mechanics*. Pergamon Press, Oxford.

[19] Patrick Le Tallec, (1990) *Numerical Analysis of Viscoelastic Problems.* Springer-Verlag, Berlin.

[20] Ahid D. Nashif, David I. G. Jones and John P. Henderson (1985) *Vibration Damping*. John Wiley & Sons, New York.

[21] Allen C. Pipkin, (1972) *Lectures on Viscoelasticity Theory*. Springer-Verlag, Berlin.

[22] Walter T. Read, (1950) "Stress analysis for compressible viscoelastic materials," *Journal of Applied Physics* **21**:671-674.

[23] Marcus Reiner, (1971) *Advanced Rheology*. H. K. Lewis, London.

[24] Michael Renardy, William J. Hrusa and John A. Nohel (1987) *Mathematical Problems in Viscoelasticity*. Longmans Scientific and Technical Press, Burnt Mill, UK.

[25] Nicholas W. Tschoegl, (1989) *The Phenomenological Theory of Linear Viscoelastic Behavior: An Introduction.* Springer, New York.

[26] G. V. Vinogradov, and A. Ya. Malkin (1980) *Rheology of Polymers: Viscoelasticity and Flow of Polymers*. Mir Publishers, Moscow.

[27] Alan S. Wineman, and Kumbakonam R. Rajakopal (2000) *Mechanical Response of Polymers – An Introduction.* Cambridge, New York.

[28] Craig G. Merrett, and Harry H. Hilton (2015) "Fractional order derivative aero-servo-viscoelasticity," *International Journal of Dynamics and Controls* **3**:1–14.

[29] Cecile Coussot, Sureshkumar Kalyanam, Rebecca Yapp and Michael F. Insana (2009) "Fractional derivative models for ultrasonic characterization of polymer and breast tissue viscoelasticity," *IEEE Transactions on Ultrasonics, Ferroelectrics, and Frequency Control* **56**:715–726.

[30] Sundaram Gunasekaran, and M. Mehmet Ak (2003) *Cheese Rheology and Texture.* CRC Press, Boca Raton.

[31] Anonymous (1951) *ANC–5, Strength of Metal Aircraft Elements.* US Government Printing Office, Washington. DC.

[32] Harry H. Hilton, and Morey Feigen (1960) "Minimum weight analysis based on structural reliability," *Journal of the Aero/Space Sciences* **27**:926–934.

[33] Harry H. Hilton,and S. T. Ariaratnam (1994) "Invariant anisotropic large deformation deterministic and stochastic combined load failure criteria," *International Journal of Solids and Structures* **31**:3285–3293.

[34] Francis R. Shanley, and Ryder, E. I. (1937) "Stress ratios: The answer to the combined loading problem," *Aviation* **36**: 28–29, 43, 66, 69–70.
[35] Bisplinghoff, Raymond L., Holt Ashley and Robert L. Halfman (1955) *Aeroelasticity.* Addison-Wesley Publishing Company, Cambridge, MA. (1980) Dover Publications, New York.
[36] Parkus, Heinz and Josef L. Zeman (1970) "Some stochastic problems in thermoviscoelasticity," *Proceedings IUTAM Symposium on Thermoinelasticity.* 226–240, Springer, New York.
[37] Pierre-Simon, Marquis de Laplace, (1846) *Théorie analytique des probabilités. Œvres de Laplace.* Vol. 5. Imprimerie Royale. Paris.
[38] Andrey N. Kolmogorov, (1956) *Foundations of the Theory of Probability.* Chelsey Publishing Co., New York.
[39] Mark J. Schervish, (1995) *Theory of Statistics.* Springer, NewYork.
[40] Douglas C. Montgomery, and George C. Runge (2007) *Applied statistics and probability for engineers.* 4^{th} ed., Wiley, Hoboken, NJ.
[41] Robert V. Hogg, and Allen T. Craig (1995) *Introduction to Mathematical Statistics.* 5^{th} ed., Prentice Hall, Edgewood Cliffs, NJ.
[42] Ronald A. Fisher, (1922) "On the mathematical foundations of theoretical statistics," *Philosophical Transactions of the Royal Society, Series A* **222**:309–368.
[43] Ronald A. Fisher, . (1925) "Theory of statistical estimation," *Proceedings of the Cambridge Philosophical Society* **22**:700–725.
[44] Ronald A. Fisher, (1934) "Two new properties of mathematical likelihood," *Proceedings of the Royal Society, Series A* **144**:285–307.
[45] Papoulis, Athanasios and S. Unnikrishna Pillai (2002) *Probability, Random Variables and Stochastic Processes.* McGraw-Hill, New York.
[46] Stigler, Stephen (1973) "Studies in the history of probability and statistics. XXXII: Laplace, Fisher and the discovery of the concept of sufficiency," *Biometrika* **60**:439–445.
[47] A. S. Kholevo, (2001) "Sufficient statistic," *Encyclopedia of Mathematics*, Michael Hazewinkel, Ed., Springer, Berlin.
[48] Yu-Kweng Lin, (Mike) (1967) *Probabilistic Theories of Structural Dynamics.* McGraw-Hill Book Co., New York.
[49] Waloddi Weibull, (1951) "A statistical distribution function of wide applicability," *ASME Journal of Applied Mechanics* **18**: 293–297.
[50] Harry H. Hilton, Michael Michaeli, Abraham Shtark, Hagay Grosbein, Eli Altus, Jutima Simsiriwwong and Rani W. Sullivan (2017) *Probabilistic Characterizations of Linear Isotropic Viscoelastic Properties from 1–D Statistical Quasi-static Tensile and Dynamic Compressive Experiments.* To be submitted to Springer, Berlin.
[51] Harry H. Hilton, John Hsu and John S. Kirby (1991) "Linear viscoelastic analysis with random material properties," *Journal of Probabilistic Engineering Mechanics* **6**:57–69.
[52] Harry H. Hilton, and Sung Yi (1993) "Stochastic viscoelastic delamination onset failure analysis of composites," *Journal of Composite Materials* **27**:1097–1113.
[53] R. A. Larder, and C. W. Beadle (1976) "The stochastic finite element simulation of parallel fiber composites," *Journal of Composite Materials* **10**:21–31.
[54] Elishakoff Isaac (1999) *Probabilistic Theory of Structures*. Dover, Mineola, NY.
[55] M. Jiang, K. Alzebdeh, Iwona M Jasiuk and Martin Ostoja-Starzewski (2001) "Scale and boundary conditions effects in elastic properties of random composites," *Acta Mechanica* **148**:63–78.
[56] Simsiriwong, Jutima, Rani W. Sullivan, Harry H. Hilton and Daniel Drake (2012) "Statistical analysis of creep compliance of vinyl ester resin," *Proceedings Fifty-third AIAA/ASME/ASCE/*

AHS/ASC Structures, Structural Dynamics and Materials (SDM) Conference, AIAA Paper 2012-1730.

[57] Simsiriwong, Jutima, Drake Drake, Rani W. Sullivan and Harry H. Hilton (2012) "A parametric study of the statistical parameters of creep compliance of a vinyl ester polymer," *Proceedings of 27 rd Technical Conference of the American Society for Composites* Arlington, TX.

[58] Simsiriwong, Jutima, Rani W. Sullivan, Thomas E. Lacy and Harry H. Hilton (2013) "Viscoelastic creep compliance of a vinyl ester polymer with statistical distribution functions," *Proceedings American Society for Composites 28th Technical Conference,* (Charles Bakis, ed.), University Park, PA.

[59] Tuegel, Eric J., Robert P. Bell, Alan P. Berens, Thomas Brussat, Joseph W. Cardinal, Joseph P. Gallagher, and James Rudd (2013) "Aircraft structural reliability and risk analysis handbook, Volume 1: Basic Analysis Methods," *USAF Report AFRL-RQ-WP-TR-2013-0132.*

[60] Simsiriwong, Jutima (2014) "Statistical characterization of viscoelastic creep compliances of a vinyl ester polymer," *Ph. D. Thesis in Aerospace Engineering,* Mississippi State University.

[61] Simsiriwong, Jutima, Rani W. Sullivan and Harry H. Hilton (2014) "Master creep compliance curve for random viscoelastic material properties," *Challenges In Mechanics of Time-Dependent Materials and Processes in Conventional and Multifunctional Materials* **2**:41–47, Springer, Berlin.

[62] Simsiriwong, Jutima, Rani W. Sullivan, Thomas E. Lacy, Jr. and Harry H. Hilton (2015) "A statistical approach to characterize the viscoelastic creep compliances of a vinyl ester polymer," *Polymer Testing Journal* **48**:183–198.

[63] Emri, Igor and Nicholas W. Tschoegel (1993) "Generating line spectra from experimental responses. Part I: Relaxation modulus and creep compliance," *Rheological Acta* **32**:311–321.

[64] Nicolas W. Tschoegel, and Igor Emri (1993) "Generating line spectra from experimental responses. Part II: Storage and loss functions," *Rheological Acta* **32**:322–327.

[65] Werner Kuhn, (1939) "Elastizität und Viscosität hochpolymerer Verbindungen," *Angewandte Chemie* **52**:289–301. doi: 10.1002/ange.19390521602

[66] Alfred M. Freudenthal, and B. Albrecht (1958) "On relaxation spectra in high polymers," *Transactions Society of Rheology* **2**:95.

[67] Rani W. Sullivan, (2012) "Using a spectrum function approach to model flexure creep in viscoelastic composite beams," *Mechanics of Advanced Materials and Structures* **19**:39–47.

[68] Rani W. Sullivan, (2008) "Development of a viscoelastic continuum damage model for cyclic loading," *Mechanics of Time-Dependent Materials* **12**:329–342.

[69] Rani W. Sullivan, (2003) "An analytical method to determine the mechanical properties of linear viscoelastic solids," *Ph. D. Dissertation*. Mississippi State University.

[70] Rani W. Sullivan, (2006) "On the use of spectrum-based model for linear viscoelastic materials," *Mechanics Time-Dependent Materials* **10**:215–238.

[71] F. Schwarzl, and A. J. Staverman (1952) "Higher approximation methods for the relaxation spectrum from static and dynamic measurements of viscoelastic-elastic materials," *Applied Scientific Research* Section A, **4**:127–141.

[72] F. Schwarzl, and A. J. Staverman (1952) "Higher approximations of relaxation spectra," *Physica* **18**:791–798.

[73] Harry H. Hilton, Jutima Simsiriwwong and Rani Warsi Sullivan Hilton (2017) "Analytical and experimental probabilistic constitutive relation characterizations. Part II: Nonlinear viscoelastic media," to be submitted to *International Journal of Mathematics in Engineering, Science and Aerospace (MESA).*

[74] Abramowitz, Milton and Irene A. Stegun (1964) *Handbook of Mathematical Functions.* National Bureau of Standard, Washington, DC.

[75] Granino A. Korn, and Theresa M. Korn (1968) *Mathematical Handbook for Scientists and Engineers.* McGraw-Hill, New York..

[76] Harry H. Hilton, (2017) "Elastic and viscoelastic Poisson's ratios: The theoretical mechanics perspective," *International Journal of Materials Science and Applications* **8**:291–332.

[77] Prony, Gaspard C. F. M. R., Baron de (1795) "Essai experimental et analytique," *Journal de l'École Polytechnique de Paris* **1**:24–76.

[78] Johann E. Wiechert, (1893) "Gesetze der elastischen Nachwirkung für konstante Temperatur," *Annalen der Physik und Chemie* **50**:335–348.

[79] Legendre, Adrien-Marie (1805) *Nouvelles méthodes pour la détermination des orbites des comètes.* F. Didot, Paris.

[80] Emil L. Post, (1930) "Generalized differentiation," *Transactions of the American Mathematical Society* **32**:723–781.

[81] Ronald L. Bagley, and Peter J. Torvik (1979) "A generalized derivative model for an elastomer damper," *Shock and Vibration Bulletin* **49**:135–143.

[82] Rogers, Lynn (1983) "Operators and fractional derivatives for viscoelastic constitutive equations," *Journal of Rheology* **27**:351–372.

[83] Mainardi, Francesco (2010) *Fractional Calculus and Waves in Linear Viscoelasticity: An Introduction to Mathematical Models.* Imperial College Press, London.

[84] Namsrai, Khavtgai (2016) *Universal Formulas in Integral and Fractional Differential Calculus.* World Scientific, New York.

[85] Harry H. Hilton, (2012) "Generalized fractional derivative anisotropic viscoelastic characterization," *Materials* **5**:169–191.

[86] Freed, Allan, Kai Diethelm and Yury Luchko (2002) "Fractional–order viscoelasticity (FOV): Constitutive development using fractional calculus: First annual report," *NASA TM-2002-211914.*

[87] Tom T. Hartley, and Carl F. Lorenzo (1998) "A solution to the fundamental linear fractional order differential equation," *NASA TP-1998-208693.*

[88] A, Chatterjee, (2005) "Statistical origins of fractional derivatives in viscoelasticity," *Journal of Sound and Vibrations* **284**:1239-1245.

[89] Caputo, Michele (1967) "Linear model of dissipation whose Q is almost frequency independent-II," *Geophysical Journal Royal Astronomical Society* **13**:529–539.

[90] Ferry, John D. (1980) *Viscoelastic Properties of Polymers.* John Wiley & Sons, New York.

[91] Malcolm E. Williams, Robert F. Landel and John D. Ferry (1955) "The temperature dependence of relaxation mechanisms in amorphous polymers and other glass-forming liquids," *Journal American Chemical Society* **77**:3701–3707.

[92] Robert F. Landel, (2005) "A two-part tale: the WLF equation and beyond linear viscoelasticity," *Journal of Rubber Chemistry and Technology* **79**:381–401.

[93] Harry H. Hilton, and Hal G. Russell (1961) "An extension of Alfrey's analogy to thermal stress problems in temperature dependent linear viscoelastic media," *Journal of Physics and Solids* **9**:152–164.

[94] Harry H. Hilton, and James R. Clements (1964) "Formulation and evaluation of approximate analogies for temperature dependent linear viscoelastic media," *Thermal Loading and Creep* **6**:6-17–6-24, Institution of Mechanical Engineers, London.

[95] Harry H. Hilton, (2011) "Equivalences and contrasts between thermo-elasticity and thermo-viscoelasticity: a comprehensive critique," *Journal of Thermal Stresses* **34**:488–535.

[96] S. Richard Turner, (1973) "Creep in glassy polymers," *The Physics of Glassy Polymers.* (Leslie Holliday, A. Kelly, Robert N. Haward, Eds.) 223–278. Wiley, NewYork.

[97] Jonathan A. Gimbel, Joseph J. Starver and Louis J. Soslowsky (2004) "The effect of overshooting the target strain on estimating viscoelastic properties from stress relaxation experiments," *Journal of Biomechanical Engineering* **126**:844–848.

[98] Harry H. Hilton, (1996) "On the inadmissibility of separation of variables solutions in linear anisotropic viscoelasticity," *International Journal of Mechanics of Composite Materials and Structures* **3**:97–100.

[99] Cristina E. Beldica, and Harry H. Hilton (2017) "Analytical and computational simulations of experimental determinations of deterministic and random linear viscoelastic constitutive relations," accepted for publication *Journal of Sandwich Structures and Materials.* (1999) *Proceedings of the Twelfth International Conference on Composite Materials (ICCM-12)* **CD-ROM Vol.**:346–371, Paris.

[100] Wolfgang G. Knauss, and J. Zhao (2007) "Improved relaxation time coverage in ramp-strain histories," *Mechanics of Time-Dependent Materials* **11**:199–216.

[101] Harry H. Hilton,(2016) "Nonlinear elastic and viscoelastic 1–D wave propagation modeling and analysis," *International Journal of Mathematics in Engineering, Science and Aerospace (MESA)* **8**:301–332.

[102] Shtark, Abraham, Hagay Grosbein, G. Sameach and Harry H. Hilton (2007) "An alternate protocol for determining viscoelastic material properties based on tensile tests without use of Poisson ratios," *Proceedings of the 2007 International Mechanical Engineering Congress and Exposition. ASME Paper IMECE2007-41068*.

[103] Shtark, Abraham, Hagay Grosbein and Harry H. Hilton (2009) "Analytical determination without use of Poisson ratios of temperature dependent viscoelastic material properties based on uniaxial tensile experiments," *Proceedings of the 2009 International Mechanical Engineering Congress and Exposition. ASME Paper IMECE2009-10332*.

[104] Michaeli, Michael, Abraham Shtark, Hagay Grosbein, Andrew J. Steevens and Harry H. Hilton (2011) "Analytical, experimental and computational viscoelastic material characterizations absent Poisson's ratios," *Proceedings Fifty-Second AIAA/ASME/ASCE/AHS/ ASC Structures, Structural Dynamics and Materials (SDM) Conference, AIAA Paper 2011-1809*.

[105] Michael Michaeli, Abraham Shtark, Hagay Grosbein and Harry H. Hilton (2012) "Characterization of isotropic viscoelastic moduli and compliances from 1-D tension experiments," *Proceedings Fifty-Third AIAA/ASME/ASCE/AHS/ASC Structures, Structural Dynamics and Materials (SDM) Conference, AIAA Paper 2012-1574.* Honolulu, HI.

[106] Michaeli Michael, Abraham Shtark, Hagay Grosbein, Eli Altus and Harry H. Hilton (2014) "Analytical and experimental protocols for unified characterizations in real time space for isotropic linear viscoelastic moduli from 1–D tensile experiments," *Challenges in Mechanics of Time-Dependent Materials and Processes in Conventional and Multifunctional Materials* **2:**75-81. Springer, New York.

[107] Michael Michaeli, Abraham Shtark, Hagay Grosbein, Eli Altus and Harry H. Hilton (2013) "A unified approach to characterization of isotropic linear viscoelastic moduli and compliances directly from 1-D tensile experiments," *Proceedings Fifty-fourth AIAA/ ASME/ASCE/AHS/ASC Structures, Structural Dynamics and Materials (SDM) Conference, AIAA Paper 2013-1692*, Boston, MA.

[108] Michael Michaeli, Abraham Shtark, Hagay Grosbein, Eli Altus and Harry H. Hilton (2014) "Uncertainty in characterizations of linear viscoelastic properties from 1 – D tensile and dynamic experiments," *Proceedings Fifty-fifth AIAA/ASME/ASCE/AHS/ASC Structures, Structural Dynamics and Materials (SDM) Conference, AIAA Paper 2014-0506*, National Harbor, MD.

[109] ASTM Committee D20.10 (2016) "Standard test method for tensile properties of plastics," *ASTM Book of Standards* **08.01**.

[110] Pfanzagl, Johann (1994) *Parametric Statistical Theory.* Walter de Gruyter, Berlin.

[111] R. Zak, Adam (1967) "Structural analysis of realistic solid propellant materials," *Journal of Spacecraft and Rockets* **5**:270-275.

[112] Taylor, Robert L., Karl L. Pister and Gerald L. Goudreau (1970) "Thermomechanical analysis of viscoelastic solids," *International Journal for Numerical Methods in Engineering* **2**:45-59.

[113] Harry H. Hilton, and Sung Yi (1993) "Anisotropic viscoelastic finite element analysis of mechanically and hygrothermally loaded composites," *Composites Engineering* **3**:123-135.

[114] Yi, Sung and Harry H. Hilton (1994) "Dynamic finite element analysis of viscoelastic composite plates in the time domain," *International Journal for Numerical Methods in Engineering* **37**:4081-4096.

[115] Yi, Sung, Shih Fu Ling, Ming Ying, Harry H. Hilton and R. Jack Vinson (1999) "Finite element formulation for anisotropic coupled piezo-hygro-thermo-viscoelasto-dynamic problems," *International Journal of Numerical Methods in Engineering* **45**:1531-1546.

[116] J. Barbero, Ever (2014) *Finite Element Analysis of Composite Materials Using Ansys,* 2^{nd} ed., CRC Press, Boca Raton.

[117] C. Simo, Juan and Thomas J. R. Hughes (1997) *Computational Inelasticity.* Springer, New York.

[118] Loan, Charles Van (1962) *Computational Frameworks for the Fast Fourier Transform*. SIAM, Philadelphia.

[119] Teimouri, Mahdi and Arjun K. Gupta (2013) "On the three-parameter Weibull distribution shape parameter estimation," *Journal of Data Science* **11**:403–414.